



Microstructure of West Antarctic Firn and Its Effect on Air Permeability

Ursula Rick and Mary Albert

September 2004

ERDC/CRREL TR-04-16
September 2004

Microstructure of West Antarctic Firn and Its Effect on Air Permeability

Ursula Rick and Mary Albert

Approved for public release; distribution is unlimited.

Prepared for NATIONAL SCIENCE FOUNDATION

ABSTRACT

The microstructure of snow and firn has a great impact on the transport of chemical species from the atmosphere to the underlying firn. For improved ice core interpretation, it is important to understand air-snow interactions within the firn layers and how they are affected by snow microstructure. Permeability and thick-section microstructure measurements have been made from snowpit and firn core samples retrieved during the U.S.–International Trans-Antarctic Science Expedition (ITASE) 1999–2001 field seasons. Our measurements have shown that the permeability of the snow at all of the sites generally increases with depth into the firn to about 3 m, then decreases due to microstructure changes, although at several sites there were areas of increased permeability at depth because of local changes in weather and climate. Thick-section microstructure measurements show that the grain size generally increases with depth, and the specific surface decreases with depth. Rapid grain growth is caused by diurnal and seasonal temperature gradients near the surface. Deeper in the core, the grain growth slows as the firn temperature gradients become small. The grain growth and specific surface trends do not follow those of the permeability. Pore size correlates well with the permeability of the snow samples; a formula was developed that predicts the firn permeability from pore characteristics. In addition to variation with depth in the core, the permeability and microstructure vary greatly from site to site, revealing that meteorological effects, such as accumulation rate and mean annual temperature, are important factors in shaping the firn microstructure. High accumulation rates or low mean annual temperatures will result in low permeability due to little or no metamorphism in the firn, although accumulation rate seems to be the dominant factor. Conversely, high mean annual temperatures cause faster grain growth, and low accumulation rates leave the near-surface firn exposed to temperature gradients for a longer time. Competing effects of temperature and accumulation rate can result in similar densities for sites of very different meteorological conditions. However, the permeability profile is a more sensitive indicator of meteorological condition than density. Physical characteristics of permeability and microstructure in the firn serve as climate indicators.

DISCLAIMER: The contents of this report are not to be used for advertising, publication, or promotional purposes. Citation of trade names does not constitute an official endorsement or approval of the use of such commercial products. All product names and trademarks cited are the property of their respective owners. The findings of this report are not to be construed as an official Department of the Army position unless so designated by other authorized documents.
DESTROY THIS REPORT WHEN IT IS NO LONGER NEEDED. DO NOT RETURN TO THE ORIGINATOR.

CONTENTS

1	INTRODUCTION.....	1
2	BACKGROUND.....	4
	Ice Cores and Climate Change.....	4
	Near-Surface Processes.....	5
	Applications to Atmospheric Chemistry.....	6
	Snow and Firn Microstructure.....	8
	Transport/Microstructure Relationships.....	10
	Our Research Project.....	11
3	METHODS.....	12
	ITASE Firn Core Information.....	12
	Stratigraphy.....	13
	Density.....	14
	Permeability.....	14
	Quantitative Microscopy.....	16
	Image Processing.....	18
4	MEASUREMENTS.....	24
	Stratigraphy.....	24
	Density and Porosity.....	25
	Permeability.....	25
	Microstructure.....	28
5	DISCUSSION.....	37
	Temperature Gradients in the Firn.....	37
	Density Increase with Depth.....	39
	Changes in Permeability with Depth.....	43
	Temporal Changes in Microstructure.....	48
	Spatial Permeability and Microstructure Variations.....	52
	Climate Indicators in Permeability and Microstructure.....	57
	Predicting Permeability from Microstructure.....	63
6	CONCLUSION.....	72
	REFERENCES.....	75

ILLUSTRATIONS

Figure 1. Schematic of the membrane sample holder used with the lab permeameter	15
Figure 2. Schematic of the field permeameter	16
Figure 3. Schematic of thick-section slices cut out of core sections	17
Figure 4. Creation of a binary image using Image Process Workbench	19
Figure 5. The same image before and after the despeckle algorithm had been applied using Image Process Workbench	20
Figure 6. Mean snow intercept length calculated by IPW before and after the despeckle algorithm had been applied	20
Figure 7. 3×3 , 5×5 , and 7×7 pixel masks for the despeckle algorithm in IPW	21
Figure 8. Ice layer from the 1999-1 firm core	24
Figure 9. Frequency and distribution of single-grained ice layers throughout the ITASE firm cores	25
Figure 10. Permeability of the ITASE firm cores from 1999, 2000, and 2001	27
Figure 11. Mean snow grain size increase with depth of the ITASE firm cores ..	29
Figure 12. Mean pore size with depth of the ITASE firm cores	30
Figure 13. Surface density of the ITASE firm cores	30
Figure 14. Specific surface of the ITASE firm cores	31
Figure 15. Permeability profile of 2000-1 core with age	32
Figure 16. Mean grain and pore intercept lengths of the homogeneous 2000-1 firm core samples.....	33
Figure 17. Mean grain and pore intercept lengths of the fine-grained 2000-1 samples only	34
Figure 18. Coarse/fine-grained sample of 2000-1 firm core	34
Figure 19. Mean grain and pore size of coarse-grained 2000-1 samples	35
Figure 20. Snow surface measurements of the 2000-1 firm core	36
Figure 21. Magnitude of temperature gradients averaged over 7 months at Siple Dome	39
Figure 22. Density increase with depth of the ITASE 1999 firm cores	41
Figure 23. Density increase with depth of the ITASE 2000 firm cores	41
Figure 24. Density increase with depth of the ITASE 2001 firm cores	42
Figure 25. Coarse-grained sample of the 2000-1 firm core at a depth of 2.5 m ..	44
Figure 26. Fine-grained sample of the 2000-1 firm core from a depth of 10.34 m	44
Figure 27. Compression stress increase throughout each firm core	46

Figure 28. Three quantitative microscopy images from fine-grained layers in the 2000-1 firn core	48
Figure 29. Growth rate of fine snow grains in the 2000-1 firn core	49
Figure 30. Specific surface decrease with time in the 2000-1 firn core	50
Figure 31. Pore size change with time	51
Figure 32. Permeability profiles of the ITASE firn cores	52
Figure 33. Comparison of mean firn grain size increase for fine-grained firn at similar ages and depths	54
Figure 34. Comparison of mean pore size at similar ages and depths	55
Figure 35. Comparison of 2001-3 firn near the surface and at 5 m	56
Figure 36. Digital images of all seven firn cores at a depth of 2 m	57
Figure 37. 2000 firn core permeability profiles illustrating multiple maxima	58
Figure 38. Mean grain intercept length increase with depth of the 2000-1 firn core	59
Figure 39. Mean pore intercept length with depth for the 2000-1 firn core	59
Figure 40. Surface characteristics with depth for the 2000-1 firn core	60
Figure 41. Images showing the abrupt increase in mean grain and mean pore sizes and the decrease in surface area	61
Figure 42. Permeability predicted by the Shimizu (1970) formula using microstructural characteristics and measured permeability	64
Figure 43. Permeability predicted by the KC equation versus measured permeability	65
Figure 44. Permeability predicted by Revil and Cathless (1999) versus measured permeability	66
Figure 45. Grain size and porosity increase with depth, which does not follow the permeability pattern of increase and then decrease	67
Figure 46. Volume-to-surface ratio of the pores in the 2000-1 firn core	67
Figure 47. Permeability predicted by Equation 22	69
Figure 48. Percent error of each sample permeability predicted by Equation 22	69
Figure 49. Permeability of 1999 firn cores predicted by Equation 22	70
Figure 50. Permeability of 2000 firn cores predicted by Equation 22	70
Figure 51. Permeability of 2001 firn cores predicted by Equation 22	71

TABLES

Table 1. Firn core site information from the ITASE field team	13
Table 2. Mean annual temperature, accumulation rate, and densification information for ITASE firn cores	40

Table 3. Compression strength range at firm densities from Abele and Gow (1975)	46
Table 4. Overburden pressure at the bottom of the ITASE firm cores	47
Table 5. Microstructure and transport properties of three fine 2000-1 firm core samples pictures in Figure 28	49

PREFACE

This report was prepared by Ursula Rick, Dartmouth College graduate student, and Mary R. Albert, Research Mechanical Engineer, U.S. Army Engineer Research and Development Center, Cold Regions Research and Engineering Laboratory. The report was originally prepared as Ursula Rick's Master's thesis at Thayer School of Engineering, Dartmouth College.

The authors thank Dr. Ian Baker and Dr. Carl Renshaw, both from Thayer School of Engineering, for their contributions. Several scientists and students at CRREL also contributed, particularly Dr. Anthony Gow, Dr. Debra Meese, Frank Perron, Jr., Susan Perron, Gina Luciano, and Merrick Johnston.

This research was supported by a grant from the National Science Foundation, Office of Polar Programs, NSF-OPP 9814676.

This publication reflects the personal views of the authors and does not suggest or reflect the policy, practices, programs, or doctrine of the U.S. Army or Government of the United States. The contents of this report are not to be used for advertising or promotional purposes. Citation of brand names does not constitute an official endorsement or approval of the use of such commercial products.

The Commander and Executive Director of ERDC is COL James R. Rowan, EN. The Director is Dr. James R. Houston.

MICROSTRUCTURE OF WEST ANTARCTIC FIRN AND ITS EFFECT ON AIR PERMEABILITY

URSULA RICK AND MARY ALBERT

1 INTRODUCTION

With the onset of global warming, it is imperative that we understand Earth's past and present climate cycles. Atmospheric conditions such as greenhouse gas budgets and dominant weather circulation patterns have been undergoing noticeable change even in the past few decades. Society must find out what part humans have had in forcing these changes and what part the natural climate cycles of Earth have had. Past climate can be reconstructed from ice cores by dating and interpreting the chemical records of the ice layers within the core. Isotope concentration, chemical species, and impurities, such as volcanic ash, indicate what sort of climate was present during the deposition of each layer and help date the ice core. It is important, then, to understand how chemical species and impurities are deposited and what changes they undergo after becoming a part of the snowpack.

Historically, ice core interpretation has been done under the assumption that the isotopes and chemistry in the ice core represent atmospheric conditions at that site when that ice was in the form of snow crystals at the surface. However, in recent years the importance of air–snow transfer processes has become apparent, as they may change the concentrations of chemical species in the surface snow before it becomes part of the deeper ice. By understanding the processes of change, we will be able to interpret signals in the ice core more accurately, leading to a better understanding of paleoclimate. Also, the flux of greenhouse and other important trace gases can be predicted more closely.

Two mechanisms that cause chemical changes in the surface snow are diffusion and ventilation. Thermal and chemical gradients cause movement by diffusion of heat, isotopes, and chemical species in the surface snow and firn (permanent snow that is compacting into ice) of an ice core. Ventilation causes interstitial air movement several meters into the snow and firn. Snow is a very good filter, collecting aerosol particles from the moving air. Thus, the movement

of air affects the aerosol record in ice cores. In addition, gases and chemical species transported by ventilation and diffusion can react with species in the snow crystals to change the concentration of both the air and the snow crystals. This has implications in atmospheric gas budgets, in addition to ice cores, as these reactions in the snow can be a sink or source for many greenhouse gases.

Ventilation is caused primarily by pressure gradients on the snow surface. These gradients force air into the snowpack and cause advection of chemical species. There are several important parameters of the snow that must be known to accurately model air movement and chemistry transport. These include diffusivity, porosity, permeability, and snow grain geometry. Permeability is the controlling transport coefficient for ventilation through the firn. The permeability of the snow can easily be measured using Darcy's Law of viscous flow through porous media. This law states that for a certain fluid, with known viscosity, at a measured fluid velocity and pressure drop, one can find the permeability of a porous material. Thus, we can find the permeability of the near-surface snow and firn of an ice core and predict the firn's propensity for ventilation.

Measuring permeability is relatively straightforward. However, the relationships between permeability and microstructure of the snowpack are not understood (Arons 1994, Albert et al. 1996, Davis et al. 1996). Airflow through firn is affected by and affects firn microstructure. Permeability depends on the nature of the interconnected pore space within the firn. This is determined by the number and geometry of pores that are connected from one end of the sample to the other, allowing air to travel the entire way through the sample. Total porosity does not take into account the interconnectedness of the pores. Ice can be very porous if it contains many air bubbles, but its permeability would be zero because the pores, or bubbles, are not connected to each other. In addition to considering density or porosity, we must use quantitative microscopy to determine other important microstructure characteristics of the firn. These measurements may then be correlated to the permeability of the firn.

This report attempts to answer several questions regarding snow microstructure and firn air permeability. First, are the permeability and microstructure similar at all ice-coring sites along the International Trans-Antarctic Science Expedition (ITASE) traverse? Will the firn microstructure vary spatially throughout Antarctica? Is permeability the same everywhere? How does microstructure contribute to this variation in permeability? If the permeability varies from place to place, then this may impact spatial variability in the preservation of chemical species. Second, how does the firn microstructure change temporally as it becomes buried and gradually turns to ice? What drives these changes in microstructure and are the driving forces the same in all places? Finally, how can we use firn microstructure to predict the permeability of the firn?

The stratigraphy, density, permeability, and microstructure of seven firn cores were measured in order to address these questions. The seven cores were obtained at ice coring sites along the ITASE traverse in West Antarctica. These cores show tremendous site-to-site differences. Microstructure and permeability vary greatly from site to site, as do the meteorological conditions. Different types of snow metamorphism can be used to explain variations in microstructure with time and in space. This change in microstructure causes changes in the permeability of the snow and firn. Measuring and understanding these variations will help us understand differences in air–snow transport processes for interpreting the ITASE ice core records.

2 BACKGROUND

Ice Cores and Climate Change

Antarctica is sensitive to and affected by climate changes around the globe. Atmospheric chemists have found evidence of volcanic eruptions from the other side of the globe in the ice of Antarctica. Antarctica holds the record of past climate in its ice layers and will tell us a great deal about the ways in which humans have introduced contaminants to our atmosphere and pushed climate change. However, the linked systems are complicated, and we must first understand the current atmospheric conditions, climate, and processes of change if we are to understand patterns from the past. Only then may we be able to reverse or ease anthropogenic effects.

To understand the Antarctic climate, scientists have drilled ice cores and analyzed the layers through the depth of the core. Drilling an ice core is a bit like using tree rings to date a tree. Because of the extreme cold at Antarctic latitudes, yearly accumulation never melts completely at many places on the Antarctic ice cap. Therefore, layers of snow build up with time, and each layer is caused by a depositional event (Alley 1988). In some areas the ice cap is nearly 4000 m thick. By drilling an ice core, scientists can see the yearly layers to date the core and estimate the chemical concentrations to find cycles in atmospheric chemistry. The first ice cores drilled were only hundreds of meters thick. Within the last 15 years, deep cores have been drilled all the way to bedrock in several areas of Antarctica and in the Arctic. The Vostok core reached an eventual length of 3350 m, and its layers date back nearly 400,000 years (Petit et al. 1997). The Siple Dome core was 1000 m thick and contained layers from as far back as 100,000 years (Nereson et al. 1996). The GRIP and GISP2 deep ice cores from Greenland reached bedrock around 3000 m and dated back about 110,000 years [Greenland Summit Ice Cores, *Journal of Geophysical Research*, 102(C12), 1997].

Several kinds of data are used to date ice cores: (1) impurities, such as volcanic ash, in the ice, (2) the isotopic and chemical composition of the ice itself, and (3) air trapped in the gas bubbles. Impurities deposited with the snow grains come from the original deposition event and are not highly volatile. Thus, an impurity, such as volcanic ash, can be used to date its layer based on the eruption time and the time required for the ash to travel from the known volcano site. However, the air bubbles and chemical species concentrations found in a particular layer do not necessarily match those found in the atmosphere at the time of that layer's deposition.

Data indicate that gas and chemical species movement by diffusion and ventilation through the top layers of snow can significantly alter the record of gases and particles in the ice core (Gjessing 1977, Cunningham and Waddington 1993). Ventilation will also affect the age of the air in the bubbles below pore close-off, as air bubble compositions do not correspond directly to the time the layer was deposited. Schwander et al. (1988, 1993) found that air exchange with the atmosphere occurs down to a depth of roughly 70 m in the GRIP core and the Siple Station core. This means the air that is eventually trapped in the bubbles is significantly younger than the surrounding ice of that layer. In the case of GRIP, the air at 70 m was 210 years younger than the surrounding snow (Schwander et al. 1993). Post-depositional change by near-surface processes affects the chemical species profiles measured in an ice core and makes dating of the ice core more complicated.

Near-Surface Processes

In actuality, the top tens of meters of an ice core are composed of snow and firn, not solid ice. Firn is simply snow that has never melted through the years and is being compacted into ice. With time and pressure, the porous firn is compressed into ice with entrapped air bubbles. The depth at which the firn becomes ice is called the firn–ice transition or pore close-off. As the name implies, it is the depth at which the network of pores between snow grains becomes discrete air bubbles within the ice. The firn–ice transition usually takes place around 50–80 m (Gow et al. 1997, Gow 1968) and is indicated when the firn density becomes equal to that of ice with 10% by volume air bubbles, about 830 kg/m^3 . At even greater depths, the bubbles are squeezed smaller and are forced to move to the grain boundaries and triple junctions in the ice.

The firn–ice transition depth varies from site to site because of temperature, accumulation rate, and any strain caused by ice flow.* As temperature increases, metamorphism of the snow grains becomes more rapid. This will result in faster densification and a shallower firn–ice transition. Accumulation rate affects the densification of snow grains by controlling the amount of metamorphosis. Higher accumulation results in faster burial of surface snow and less time spent in the near-surface firn, where temperature gradients are greatest. Thus, there will be less metamorphosis caused by temperature gradients. This slows the snow's rate of densification and lowers the firn–ice transition. Increased strain caused by ice flow will increase the rate of densification. The strain phenomenon is evident in the Upstream B ice core, collected on the Siple Coast, which had a firn–ice transition of 33 m (Alley and Bentley 1988), one of the shallowest ever recorded.

* Personal communication with Dr. Anthony Gow, CRREL, 2002.

There are three zones of transport in an ice core (Sowers et al. 1992): convection in the top several meters, diffusion through the pore space between the convection zone and pore close-off, and then diffusion through the ice below pore close-off. Transport of chemical species by diffusion through the air space can occur down to the firn–ice transition depth. The top meters of snow are sufficiently permeable to allow airflow and advection of chemical species by wind-driven ventilation (Albert et al. 2002).

Diffusion is driven by thermal or chemical gradients, and it may occur across individual snow grains, from the snow grains to the interstitial air, or across the air space. However, diffusion is a very slow process and alone is not enough to explain the movement of chemical species through snow and firn. Traditionally, ice core interpretation used the assumption that diffusion was the only mechanism controlling gas and chemical species movement within an ice core (Schwander et al. 1993), but Albert (1996) determined from modeling that estimates of chemical transport by diffusion alone would be lower than the actual amount of transport. Advection must also control mass movement within the firn by ventilation of air through the firn.

Ventilation, or wind pumping, is a result of pressure variations over the snowpack. Atmospheric pressure changes cause a slow, “breathing” of the firn but do not cause enough flow to affect thermal or chemical conditions in the firn. Turbulent wind conditions can also cause ventilation of air into the snow by eddy movement on the snow surface. These are relatively small pressure perturbations and would only affect the top several centimeters of the firn. The most important cause of surface pressure changes is surface roughness. High pressure on the windward side of a sastrugi and low pressure on the leeward side cause strong pressure gradients over the snow. These conditions result in vertical flow of atmospheric air into the snowpack and lateral flow within the snowpack, thus advecting heat or chemical species throughout the snowpack (Clarke and Waddington 1991, Colbeck 1989, 1997, Albert 1993, 1996). Ventilation depends on both the nature of the snow (Albert et al. 1996, Albert and Hawley 2000, 2002) and the driving forces and may drive chemical species and heat down to several meters at some sites. Ventilation also causes sublimation of the snow, which will affect mass balance over the snow, chemical species migration, and the physical properties of the snow (Albert 2002).

Applications to Atmospheric Chemistry

The transport of air and chemical species through snow is also of importance for atmospheric chemistry studies over snowpacks. Snow plays a significant role in the chemistry of the atmosphere above it. Recent research in polar regions, as

well as at midlatitudes, has demonstrated that snow can act both as a sink and as a source for many trace gases that are of importance for atmospheric composition and chemistry.

Chemical species are deposited in the snowpack by one of three deposition mechanisms: wet, fog, or dry deposition (Davidson et al. 1996). In addition, reactions in the snowpack can change various chemical species and concentrations. Wet deposition occurs when snow scavenges gases and aerosols while falling to earth. Fog deposition is similar to wet deposition in that gases and aerosols are scavenged, but by water droplets instead of ice crystals; when the water vapor condenses at the surface of the snow in the form of surface hoar, the chemical species within the water droplet become part of the snowpack. Dry deposition is continuously occurring by three steps, even if there is no precipitation occurring over the snowpack (Davidson et al. 1996). First, chemical species are transported by aerodynamic transport to the air just above the snow surface by wind currents and chemical concentration gradients. Second, boundary layer transport causes particles and gases to move from the air onto the snowpack surface by gravity, diffusion, and impaction of the species with the surface. Finally, surface interactions determine whether the particle or gas will remain a part of the snowpack. Snow is a very good filter and removes nearly all of the particles in the air (Harder et al. 1996). The amount of ventilation will greatly affect the number of particles collected by the snow. Also, particles may dissolve if there is a layer of water on the snow grains, or they may bounce off if the surface is dry. Soluble gases will dissolve into the snow, while insoluble gases will remain part of the air currents (Davidson et al. 1996).

Once gases and aerosols build up in the snow, they move to and from the atmosphere according to their reactivity and meteorological conditions such as temperature, amount of sunlight, and relative humidity. The list of compounds that have been found to actively exchange between snow and the atmosphere includes species such as nitrogen oxides, ozone, hydrogen peroxide, and organic compounds such as carbonyls, alkenes, and peroxy acetyl nitrate (Bottenheim et al. 2002). It has been demonstrated that these trace gas fluxes are triggered by photochemical reactions in the snow. These reactions, occurring within the snowpack, result in the release of nitrogen species, halogens, organic compounds, and hydrogen peroxide to the atmosphere (Dibb et al. 1998, 2002, Hutterli et al. 1999, Sumner and Shepson 1999, Dibb and Arsenault 2002, Honrath et al. 2002, Swanson et al. 2002). Solar irradiance was found to induce photochemical production of NO_x while consuming ozone in Antarctica and at Summit, Greenland (Honrath et al. 1999, Jones et al. 2001, Peterson and Honrath 2001). Trace gas fluxes and reactions between the snow and atmosphere are affected by snow microstructure and transport properties (Albert et al. 2002).

Snow and Firn Microstructure

The physical properties of snow have a large effect on transport within the firn. Snow rarely remains the same once it is deposited onto the surface. Any high winds will blow it around, eroding any shape the snow may have. Wind also packs the snow grains together, forming a low-permeability layer near the surface. Temperature gradients may cause the grains to grow and change shape.

It is important to note the difference between crystals and grains in snow and firn. A snow grain may be made up of more than one crystal, each with a different crystallographic orientation. Gow (1969) found that most grains are composed of one or two crystals at South Pole. He also found that grains and crystals maintain a nearly constant growth ratio near the surface. Below about 10 m the crystals grow so large that one crystal will take over its grain, and grains and crystals will become indistinguishable.

Snow grains and crystals continually undergo recrystallization. The driving force for recrystallization is the surface tension of the snow grains. Thermodynamics drives the snow grains to reduce their surface energy, so that the grains become more rounded and the large grains grow at the expense of smaller grains (Langham 1981). Below 10 m the firn experiences very small temperature gradients, so grain growth is considered isothermal and constant (Gow 1969, Colbeck 1983). Gow (1969, 1971) found at several Antarctic sites that grain growth below 10 m was linear:

$$D^2 = D_0^2 + Kt \quad (1)$$

where K = growth rate
 D^2 = grain size (mm²)
 D_0^2 = extrapolated grain size at zero time.

It must be noted that this grain size at zero time is not the real size at deposition because grains do not grow isothermally in the upper snow layers. Gow (1969) also determined that the isothermal growth rate is temperature dependent:

$$K = K_0 \cdot \exp(E/RT) \quad (2)$$

where K_0 = constant found to be 6.75×10^7 mm²/yr (Alley et al. 1982)
 E = activation energy for crystal growth, 48,570 J/mole (Gow 1969)
 R = gas constant
 T = temperature of the snow in kelvins.

The lower the temperature, the slower the snow crystals will grow.

The snow grains themselves undergo three types of metamorphism during recrystallization: dry, wet, and pressure (Langham 1981). For polar snow and firn at ice coring sites, we are mainly concerned with dry and pressure metamorphism. Wet metamorphism takes place when the snowpack is at its melting point, and liquid on the grain surface forms necks with other snow grains. This occasionally occurs near the surface in the summer in polar regions with the formation of sun crusts or monograin ice layers.

Dry metamorphism can be divided into two mechanisms: equitemperature (ET) and temperature gradient (TG) metamorphism (Colbeck 1982, 1983). As the name implies, ET metamorphism takes place isothermally and causes the snow grains to grow slowly and sinter together. The primary driving forces for ET metamorphism are vapor pressure differences around the snow grains and surface tension as discussed above. Any convex surfaces on the snow grains have a higher vapor pressure than the concave surfaces. Mass transfers by sublimation from areas of high vapor pressure to areas of lower vapor pressure. Thus, the grains become more rounded as convex surfaces disappear and concave surfaces fill in. In addition to grain rounding, ET metamorphism causes sublimation from small grains to larger grains, thereby reducing the surface area of the snow and thus the free energy (Langham 1981). ET metamorphism is the dominant process in polar snowpacks below 10 m, leading to sintering of the snow grains and eventual transformation to ice. Below 10 m the firn experiences very small temperature gradients, so there are no temperature gradients strong enough to drive TG metamorphism. As in recrystallization, higher temperatures will increase the rate of ET metamorphism. The equilibrium vapor pressure of a substance will increase with temperature. As the vapor pressure increases, more vapor molecules will escape from the solid grain and redeposit elsewhere on a grain. At -40°C the vapor pressure of ice becomes zero and no water molecules can escape into the vapor phase.

Above 10 m in the firn, the temperature in the snow is not constant because of seasonal and diurnal temperature swings. In the top centimeters of snow, hourly and daily temperature changes may give rise to steep temperature gradients and TG metamorphism, which leads to rapid grain growth and destruction of the necks between snow grains (Colbeck 1982). Temperature gradients cause vapor movement through the snow from higher temperatures to lower temperatures. This vapor movement causes the growth of large-faceted crystals. These crystals are cohesionless and tend to move easily past one another. TG metamorphism is usually associated with the formation of depth hoar and very rapid crystal growth near the snow surface. Colbeck (1989) found that temperature forcing very near the surface could cause rapid grain growth. Alley et al. (1990)

found also that solar radiation was great enough to induce large temperature gradients in the top centimeters of snow, resulting in the formation of depth hoar near the surface at Summit, Greenland.

Transport/Microstructure Relationships

ET and TG metamorphism have profound effects on the transport of air through the firn. The transport properties of the snow will affect the ability of chemical species to become entrained in the snowpack, and microstructure will control the transport. Ventilation is one of the most important mechanisms of heat and mass transport into the near-surface snow, and the air permeability is the best measure of ventilation. The air permeability of snow measures the ease with which air can flow through the snow. Permeability is a material property in Darcy's Law of flow through porous media and is a required parameter when modeling movement of air through snow and firn.

Early papers on ventilation of snow assumed that the snow is a homogeneous half space with constant properties throughout its depth (Colbeck 1989, Albert 1993, Cunningham and Waddington 1993). However, the snow microstructure varies greatly, even between adjacent layers, because of metamorphism (Alley 1988) and differing depositional events. It is important to know how air flows through different types of snow and how airflow shapes the snow. Recent studies have taken into account the physical characteristics and layering of snow and how they affect air and chemical transport. Albert (1996) modeled heat, mass, and species transport in polar firn and found that layering in the snow did affect how and to what degree species moved through the firn. Low-permeability layers near the surface reduced the airflow beneath but did not completely stop flow. Despite the low-permeability layers, wind pumping can cause higher-velocity flow in underlying high-permeability layers. The model also predicted increased horizontal flow in buried high-permeability layers.

In the field both at Siple Dome, Antarctica, and at Summit, Greenland, permeability has been found to increase with depth through the first few meters of firn, but then decrease with depth (Albert et al. 2000, Albert and Schultz 2002). This increase in permeability near the surface has important implications for the amount of ventilation that can take place in the firn. It appears that the surface of polar snow in many areas has a low permeability, likely due to wind packing. However, the underlying layers with their high permeability will allow for a great deal of air transport. It is not known how widespread this permeability phenomenon is and how the profile might change from site to site.

Most efforts at relating permeability to snow microstructure have attempted to use density, porosity, and grain size to explain the changes in permeability

(e.g. Shimizu 1970). However, Albert et al. (2000) found that density is a poor indicator of permeability changes and that microstructure was controlling airflow through the snow. Hardy and Albert (1993) found no direct relationship between permeability and porosity or grain size. Some relationships between permeability and snow microstructure have been developed, but they are limited to specific snow grain types and cannot be applied broadly. Shimizu (1970) developed a formula to predict the permeability of fine-grained snow using grain size and specific gravity. This formula does not work well for polar firn, underestimating its permeability (Luciano and Albert, 2002). It would be useful to have a relationship between the microstructure of polar snow and its permeability.

Our Research Project

In recent years scientists in the ITASE project have been extracting medium-length ice cores for recent climate studies. Deep cores require a large amount of logistic support and many years to drill and analyze. If one wants to focus only on the last several hundred years of climate, medium-length ice cores can be used with a great deal less time and effort. The ITASE is employing such methods to understand Antarctic climate. By drilling several medium-length ice cores in many places, temporal, as well as spatial, climate variability can be studied. The United States' contingent of ITASE (U.S. ITASE) has been focusing on the West Antarctic Ice Sheet.

In addition to ice cores, firn cores can also be recovered in order to study the near-surface snow and firn layers. Firn cores are generally shorter than ice cores because they are only used to study the region above the firn-ice transition. Firn core drilling, atmospheric experiments, and glaciological studies have been conducted at several sites along U.S. ITASE traverses of the West Antarctic Ice Sheet. At two or three ITASE sites per year, firn cores were drilled for microstructure and air transfer studies. As of the delivery of the cores from the 2001 field season, seven firn cores had been retrieved and delivered to the Cold Regions Research and Engineering Laboratory in Hanover, N.H. These cores are used to characterize the spatial and temporal variability of the firn microstructure and also to measure the transport properties of the firn. By studying multiple sites, we will be able to better understand how the permeability varies at different places in Antarctica and how the microstructure affects air permeability. We will also be able to see the effects that weather and topography have on air-snow transport processes.

3 METHODS

ITASE Firn Core Information

The stratigraphy, permeability, and density of all of the ITASE firn cores collected during the 1999–2001 field seasons were measured. Firn cores were not drilled at every ice-coring site on the ITASE traverses but were selected at sites judged likely to represent a broad range of accumulation rates and mean annual temperatures. Two firn cores were retrieved during the 1999 and 2001 seasons, and three firn cores were drilled during the 2000 season. The naming of the cores consists of the year of the field season and the site number the firn core was taken from. Thus, the first core taken during the 1999 field season is called 1999-1.

Table 1 gives the site information for the seven ITASE cores analyzed in this study. Blue Spikes and Gordon Hamilton of the University of Maine took elevations in the field by GPS. The average accumulation rate expressed as water equivalence was measured on ice cores by Tony Gow and Debra Meese of CRREL. The accumulation rates were calculated using annual layer dating; these are preliminary as of the time of this report and still need to be compared to electrical conductivity data for improvement by Gow and Meese. The mean annual temperatures for the year 2001 were found by taking the 10-m borehole temperature. The temperature in the firn at 10 m yields a reasonable approximation of the mean annual temperature at that site because the temperature gradients between adjacent layers are very small. Above 10 m there are temperature fluctuations caused by seasonal and diurnal atmospheric temperature variations. The 1999-2 average temperature was taken from an automatic weather station (AWS) near the site. The remaining mean annual temperatures were calculated using adiabatic lapse rates.* A lapse rate of $1.15^{\circ}\text{C}/100\text{ m}$ was used to calculate the mean annual temperature of the 1999-1 site. This lapse rate was found by interpolating between Byrd Station (with an elevation of 1498 m and a mean annual temperature of -28.0°C) and the 1999-2 core (with an elevation of 935 m and a mean annual temperature of -21.5°C). The lapse rate for the 2000 cores was $0.5^{\circ}\text{C}/100\text{ m}$, again based on Byrd Station. These lapse rates are highly variable, depending on the region. Coastal regions will have different lapse rates than the Antarctic interior. Therefore, these mean annual temperatures are estimates and should only be used qualitatively.

* Personal communication with Dr. Anthony Gow, CRREL, 2003.

Table 1. Firn core site information from the ITASE field team. The location and elevation were measured by Gordon Hamilton and Blue Spikes of the University of Maine. The mean annual temperature and average annual accumulation were calculated by Tony Gow and Deb Meese of CRREL.

Core name	Location	Elevation (m)	Mean annual temperature (°C)	Ave. accum. rate (H ₂ O equiv. in cm/yr)
1999-1	80°36'S, 122°28'E	1276	-25.4 (est.)	14.7
1999-2	81°11'S, 125°54'E	935	-21.5 (AWS)	13.4
2000-1	79°23'S, 111°14'E	1790	-29.5 (est.)	17.7
2000-4	78°5'S, 120°5'W	1697	-29.0 (est.)	17.3
2000-5	77°41'S, 124°W	1828	-29.7 (est.)	11.9
2001-3	78.1°S, 95.6°W	1633	-25.9 (borehole)	33.9
2001-5	77.1°S, 89.1°W	1246	-26.4 (borehole)	36.4

Stratigraphy

ITASE firn cores were shipped to CRREL in insulated boxes containing nine 1-m sections. These were kept at -20°C during the entire shipping process from Antarctica. At CRREL the cores were stored in coldrooms of uniform temperature and maintained at -30°C . At this temperature the partial pressure of water vapor is low, so that there is little vapor transport between snow grains. Therefore, the firn microstructure remains unchanged during transport and storage.

Each firn core section was placed on a light table so that the firn layers could be easily identified. Fine-grained layers usually appear visually “dark,” and “light” layers are coarse grained. Firn layers were given a designation of coarse, fine, or coarse/fine based on their grain size relative to the surrounding layers. The purpose of identifying these layers was to resolve yearly layering patterns and determine the original snow type of specific layers (e.g. wind pack, depth hoar, etc.). Note that these are relative terms, and a coarse layer from near the top of the core may not have been designated as such if it had been found deeper in the core, since grain size increases with depth in an ice sheet. Ice layers within the core were also noted. These are thin, sometimes monograined, layers usually perpendicular to the length of the core induced by sun or wind crusting. Ice layers caused by true surface melt were rarely observed.

The core section was then cut into firn core pieces approximately 10 cm in length for measurement of permeability. At least one homogeneous fine and one homogeneous coarse sample were cut from each 1-m section. The start and end

depths of each piece were noted. Samples were placed in labeled, sealed plastic bags and stored in a -30°C coldroom until permeability tests could be conducted.

Density

The density of each firm core piece was measured in the coldroom. To find the sample volume, we measure the height and diameter of each sample with calipers to the nearest 0.01 mm. The sample was then weighed on an electronic scale to the nearest 0.1 gm. The density, ρ , was then calculated using Equation 3:

$$\rho = m / h\pi r^2 \quad (3)$$

where r = radius of the firm core piece
 h = height of the piece
 m = mass.

Some samples were not perfect cylinders because of core dog marks or sloping tops or bottoms. These deformities were noted, and the density of this sample was considered approximate.

Permeability

Permeability, k , is the property of the porous medium that relates pressure to flow rate in Darcy's Law of flow through porous media:

$$v = -\frac{k}{\mu} \frac{dP}{dx} \quad (4)$$

where v = flow rate
 P = pressure
 μ = fluid viscosity
 x = direction of fluid flow.

The air permeability of every 10-cm section of all of the firm cores was measured. Sample height, time of day, barometric pressure, and ambient temperature were noted prior to each test. The pressure drop over each core section of roughly 10 cm in length was measured at at least six flow rates per sample. Each pressure drop and flow rate pair was checked to ensure that it lay along a straight line for each core section. Any measurements not lying along this line

were out of the linear range and were not included in the averaging for permeability. The permeability values for each pair of flow rate and pressure drop in the linear range were then averaged to give an overall permeability of that core section. In general the difference between permeability values for a single sample was less than 1–2%.

The permeameter used in the lab has an elastic membrane core holder that is squeezed around the vertical edges of the firn core pieces by air pressure (Fig. 1). The elastic membrane eliminates edge effects in the firn core pieces so that no air can travel up the sides of the sample. There is a double cylinder platform on which the sample sits that also reduces edge effects. The flows are adjusted so that the pressure in each cylinder is the same. This ensures that the flow is parallel and unidirectional through the sample. A vacuum pulls air down through the sample while the pressure drop through the sample is measured.

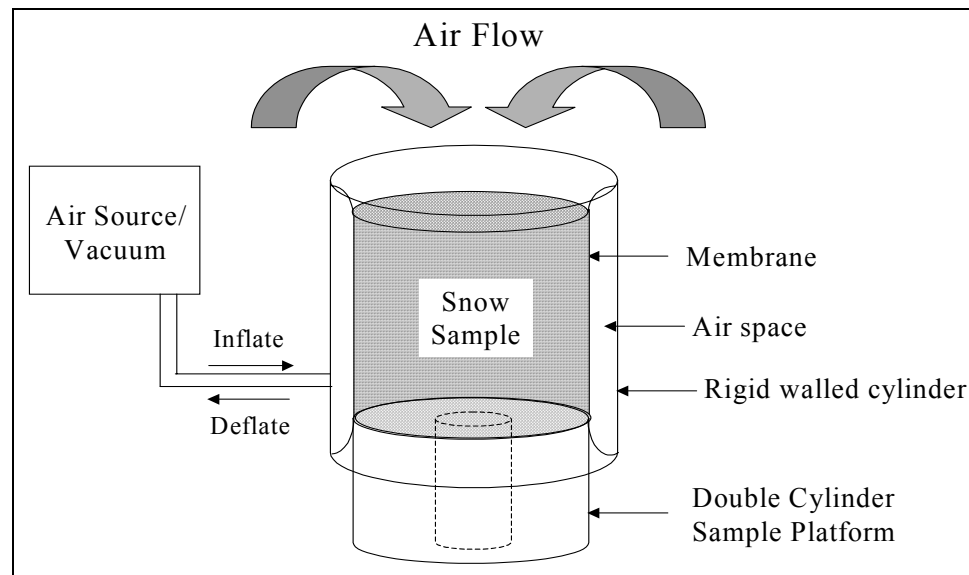


Figure 1. Schematic of the membrane sample holder used with the lab permeameter. This holder was designed to reduce flow along the sides due to imperfections caused by the coring process. Inflating the bladder between the membrane and the rigid-walled cylinder holds the sample onto the platform.

In addition to measuring the permeability of firn core pieces, measurements were taken of the top 2 m of the firn in the field. The permeameter used in the field operates under the same principle of Darcy's Law, but the design is slightly different (Fig. 2). Commonly, surface snow is measured in the field, and the snow is less sintered and more fragile to handle. The sample is contained within a

rigid, clear sample cutter with sharp teeth at the bottom for cutting through firm. A sample approximately 10 cm high was cut from a snow pit and put on a wire grate to allow for air to be pumped from beneath. The vacuum pulls the air through a double cylinder head that fits into the top of the sample holder. A double cylinder design is required because Darcy's Law assumes parallel, laminar flow (Shimizu 1970). The flows in the inner and outer cylinders can be adjusted as in the lab permeameter to ensure equal pressure within the sample and uniform parallel flow through the sample.

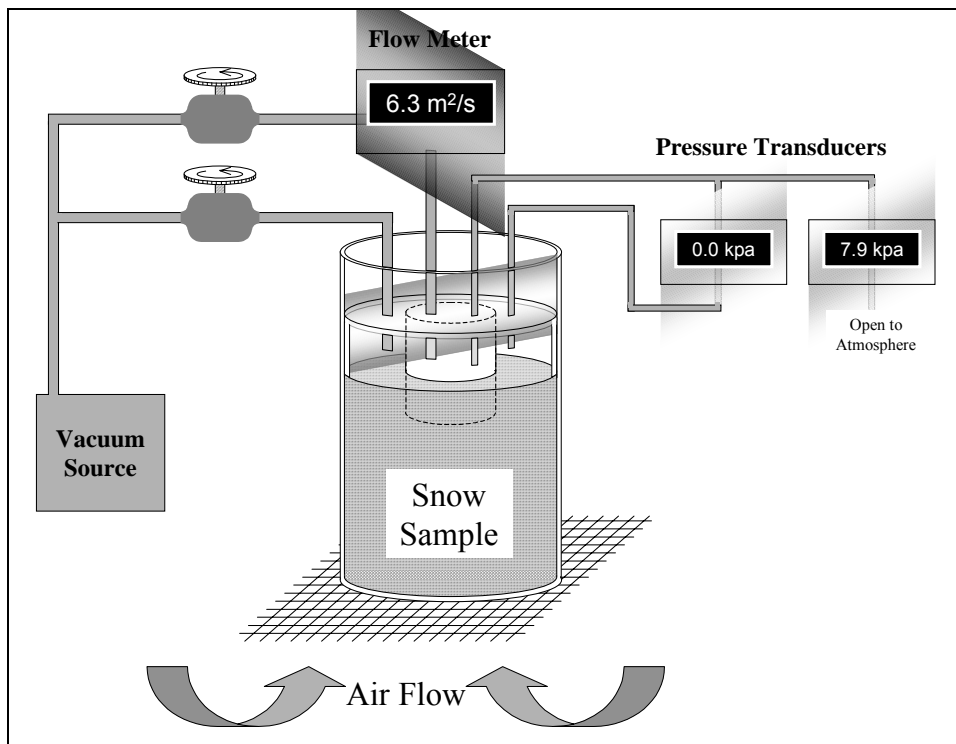


Figure 2. Schematic of the field permeameter (Albert and Schultz 2002). The sample holder is a rigid-walled container because surface field samples cut from snow pits are less cohesive.

Members of the U.S. ITASE field team made the field permeability measurements during the traverse. The data were reduced at CRREL to determine sample permeability.

Quantitative Microscopy

Only some of the firm core sections were made into thick sections for quantitative microscopy because of the time required to make and examine these sam-

ples. It is worth noting that the permeability measurements must be completed before the samples can be cut into thick sections because filling the pores and sectioning a sample for quantitative microscopy are not reversible. The permeability of that sample could not be measured afterwards. It is the goal of this work to discover the effect that microstructure has on the air permeability of polar firn. Firn core samples with more than one type of microstructure will have a permeability resulting from the combined effects of all of the layers within that sample. Therefore, only samples of homogeneous microstructure were used for stereology and quantitative microscopy. Modeling has shown that highly permeable layers, such as depth hoar, can increase lateral airflow between such layers (Albert 1996). Using core samples of one type of snow is intended to decrease the impact of layering and enable us to more clearly determine correlations between microstructure and permeability. In addition, it will enable us to examine the effect of post-depositional changes on wind pack at the various sites. Surface wind pack is ubiquitous in polar regions.

Thick-section samples were made following the procedure of Perla (1982). In a coldroom at -10°C , firn core pieces with permeabilities that had been measured were cut vertically down through the core sample so that a flat rectangular section was made (Fig. 3). Stratigraphic up was noted, and the sample was placed in a rigid-walled, plastic container. Dimethyl phthalate, a water-insoluble, organic liquid pore filler, was poured around the sample until the container was about 1/3 full. The pore filler was allowed to soak into the sample for about 10 minutes.

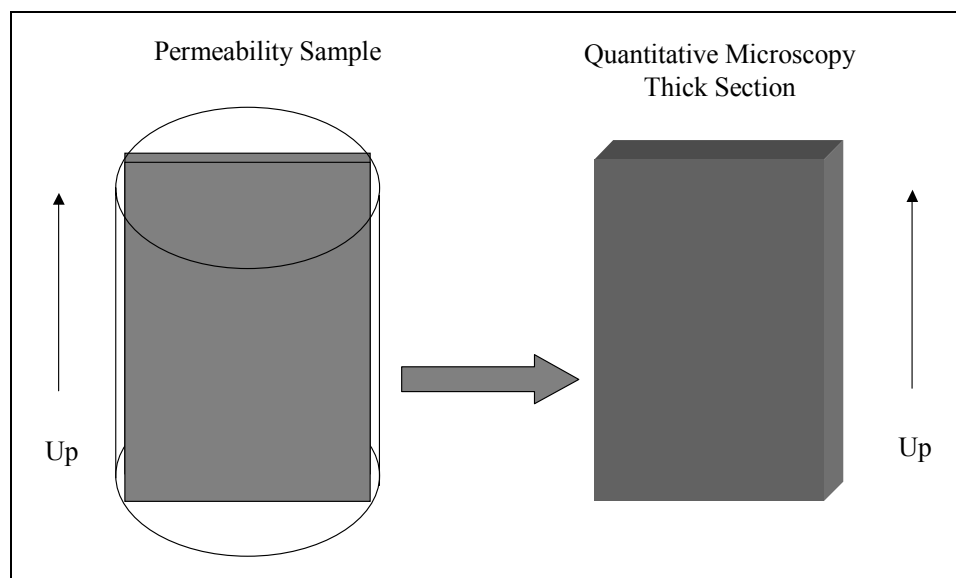


Figure 3. Schematic of thick-section slices cut out of core sections.

After adding pore filler until it reached 2/3 of the way up the sample, it was allowed to sit for another 10 minutes. More pore filler was poured in until the sample was almost completely immersed. This was allowed to sit for 30 minutes to ensure that the pore filler reached the center of the sample. Finally, the remainder of the sample was covered with the pore filler and allowed to freeze in a coldroom.

Dimethyl phthalate is a water-insoluble, organic liquid at room temperature (25°C). Its freezing point is -2°C , so the liquid at its freezing point will not melt the snow crystals in the quantitative microscopy samples. Pure dimethyl phthalate supercools to -15°C . The dimethyl phthalate is maintained at its freezing point by first freezing the entire bottle solid and then allowing some of it to melt in a warm room. While there is sufficient frozen material remaining in the container and it is well mixed, it is assumed that the liquid is at the freezing point of -2°C or lower.

Once the sample had frozen, the entire block was cut lengthwise through the center of the sample and microtomed. This was done in a coldroom at -10°C so that no surface liquid film appeared on the pore filler. For dimethyl phthalate, this surface film will appear at around -3°C (Perla 1982). The face of the sample was allowed to sublimate for about 2 days, leaving pore filler where the interstitial air had been and void where snow grains had been. Very fine-grained copier toner was then brushed on the sample face so that the voids where the snow grains had been appeared as black. The sample was then wiped level, and digital pictures were taken of the sample while in the coldroom. An image was taken of the entire microscopy sample. Then images, zoomed in to the sample, were taken for the purpose of recording a representative area of the microstructure. These images were essentially grayscale and could easily be made into a binary image for image processing.

We must know the length scale for each image. A picture is taken of a millimeter grid with the digital camera at the time the samples images are taken. These were made into a grid image for each sample taken at the same distance and focus as the sample. Using the image processing software, we could determine the number of millimeters per pixel on the grid image, which is the same as the number of millimeters per pixel on the sample image. This value is entered into Image Process Workbench (IPW) when it is asked to calculate the microstructure statistics for the sample.

Image Processing

The digital images in JPEG format were loaded into the IPW software on the CRREL Unix network. The images first had to be saved as IPW format and made

grayscale. The human eye can see at least 256 distinct grayscale levels from white to black. Thus, IPW assigns each pixel a value from 1 to 256. Then the image was thresholded and made binary (Fig. 4). The threshold limit was a designated grayscale value chosen by the software user. The threshold value was adjusted by comparing the processed image to the original digital image of the sample. Any pixels lighter gray than the threshold were made white and given a value of 1. The remaining pixels darker gray than the threshold value were made black and assigned a value of 0. Black and white was reversed during the thresholding process, so the white pixels represent regions that were snow and the black pixels represent regions that were pore space. This must be done since the IPW program considers white pixels objects and black pixels empty space in quantitative microscopy calculations.

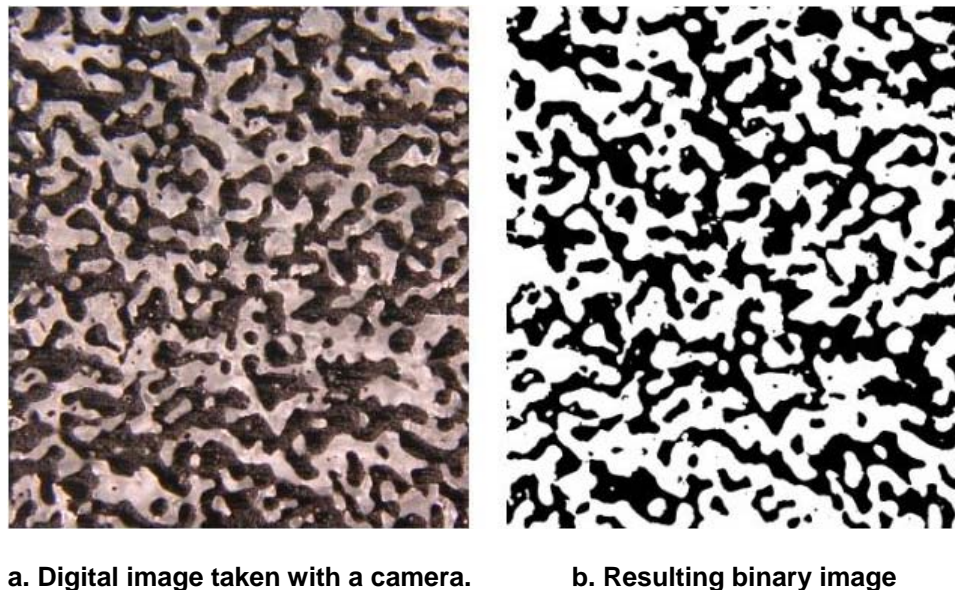


Figure 4. Creation of a binary image using Image Process Workbench.

Following the binary process, the image was smoothed using the “despeckle” algorithm in IPW. This allowed for the removal of tiny objects of a single or very few pixels in the image usually caused by glare off toner particles. Figure 5 shows an image before and after despeckling. If these tiny objects were not removed, IPW would assume they were either snow or pore space, depending on their binary specification. The image statistics for this image would not represent the true condition of the sample. Figure 6 shows how the mean grain size of the snow would be underestimated. The volume fraction of snow and the specific surface of snow would be overestimated, and it would also underestimate the

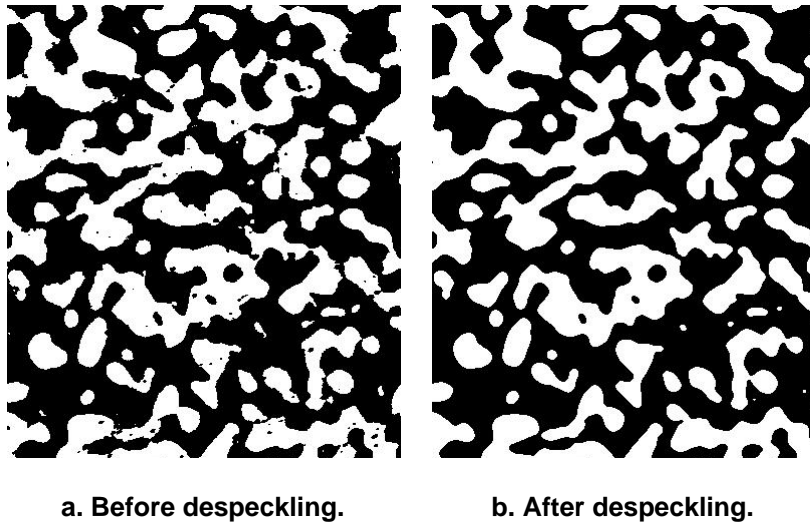


Figure 5. The same image before and after the despeckle algorithm had been applied using Image Process Workbench.

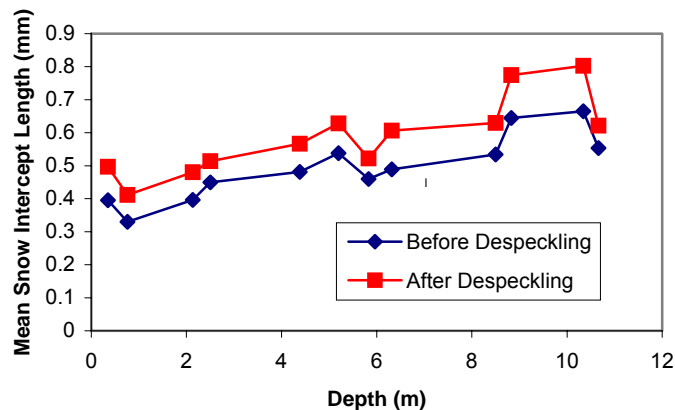


Figure 6. Mean snow intercept length calculated by IPW before and after the despeckle algorithm had been applied.

volume-to-surface ratio. Despeckling is not a perfect process and is subjective. Not all speckles could be eliminated without removing too much of the actual snow in the image. The image being despeckled was compared to the initial digital image from the camera, as in thresholding, to ensure the closest fit.

The despeckle algorithm requires the user to select 3-, 5-, or 7-pixel averaging. In the case of 3-pixel averaging, the algorithm averaged the grayscale value (0 for black, 1 for white) of the eight surrounding pixels of each pixel in the

image (Fig. 7). Then it assigned that average to the center pixel. Thus, if there was one white pixel in a background of black, the white pixel would become black. If the surrounding pixels are both black and white, then the image becomes grayscale again because the average will be between 0 and 1. To bring the image back to binary, a thresholding value of 128 (half of 256) was chosen and the image made binary. For 5-pixel averaging, the average of a 5×5 grid surrounding a center pixel was found, and the center pixel was given that average value. For 7-pixel averaging, a 7×7 grid surrounding the center pixel was averaged (Fig. 7). For our images, 7-, 5-, then 3-pixel averaging was used in that order to despeckle the images, as recommended by Robert Davis of CRREL.

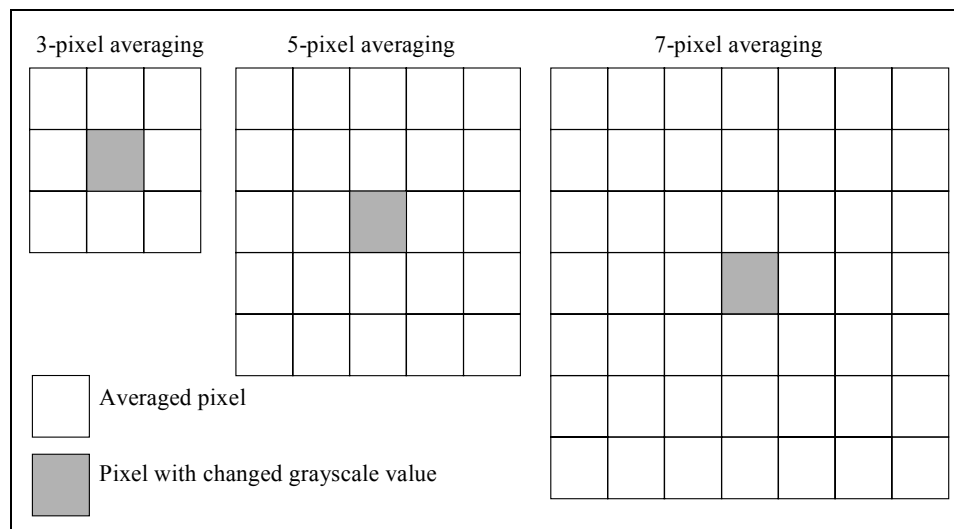


Figure 7. 3×3 , 5×5 , and 7×7 pixel masks for the despeckle algorithm in IPW. The center pixel value is changed after the surrounding pixel values are averaged.

The larger averaging grid is used first to eliminate the large “speckles.” Then progressively smaller masks are used until the single-pixel objects are removed. In the case of surface wind pack, which usually has some very small snow grains, a 5×5 mask replaced the first mask of 7×7 pixels. This ensured that no actual snow crystals were erased. This choice was made by the user and therefore is subjective.

Once the image is sufficiently processed, IPW can calculate geometrical statistics on the digital images. IPW calculates the following values for each binary image: volume density, surface density, volume/surface ratio, equivalent sphere radius, length density, mean object intercept length (mean grain size), mean object intercept area, mean object intercept volume, mean pore intercept length

(mean pore size), and maximum chord length. The most useful statistics for this research were surface density, volume/surface ratio, and mean grain and pore intercept lengths. The volume fraction of snow was calculated using Equation 5, where P is the number of pixels and V_v is the volume fraction:

$$V_v(\text{snow}) = \frac{P_{\text{snow}}}{P_{\text{total}}} . \quad (5)$$

For the remaining values, IPW uses a series of test lines, L_o , across the image. IPW uses each horizontal line of pixels in the image as a test line, so the entire image is used in calculating the statistics. The program counts the number of white pixels on each line or the number of times a boundary between snow and a pore intersects the line, depending on the image statistic desired.

Surface density is calculated by counting the number of times the test line intersects a boundary, $P_{\text{boundaries}}$, from a pore to snow:

$$S_{\text{volume}} = \frac{P_{\text{boundaries}}}{L_o} . \quad (6)$$

Thus, a sample with many small grains will have a greater surface density than one with fewer large grains. A related and important measurement is the specific surface, which is the surface density divided by the volume fraction of snow:

$$S_{\text{snow}} = \frac{S_{\text{volume}}}{V_v} . \quad (7)$$

In IPW, the inverse of the specific surface is calculated and called the volume-to-surface ratio.

The mean object intercept length, L_{snow} , which is a measure of grain size, also requires a test line across the image:

$$\bar{L}_{\text{snow}} = \frac{\sum_{N=1}^N L_N^{\text{snow}} / L_o}{N / L_o} \quad (8)$$

IPW calculates the total length of white (snow) in each line and divides that by the number of times a snow grain intersects the line, N/L_0 . The mean pore intercept length is calculated in nearly the same way except that black (pore) lengths and interceptions are used:

$$\bar{L}_{\text{pore}} = \frac{\sum_{i=1}^N L_N^{\text{pore}} / L_0}{N / L_0}. \quad (9)$$

It was also useful to determine the statistical characteristics of the pores, so the images had to be processed a second time. This involved reversing black and white so that the snow would be black and the pores white. Then the images were processed by IPW, which only considers white pixels. This would give surface density and specific surface measurements of the pores.

4 MEASUREMENTS

Stratigraphy

The data on the layer boundaries and snow grain description of each layer are archived but not reported here. The data on the number of ice layers in each firn core will be presented. The typical ice layer observed in firn cores is one or two grain diameters in thickness and most likely represents sun or wind crust. An example of such a layer can be seen near the right-hand side of Figure 8. The frequency of the ice layers in each meter of each core is plotted in Figure 9. The 1999-2 firn core had the fewest ice layers at only eight, and all of those were located in the deeper sections of the firn core. Core 1999-1 also had a relatively low number of ice layers (22). The remaining cores had between 65 and 83 layers within the entire firn core. The frequency of ice layers will become important in permeability discussions later in this report.

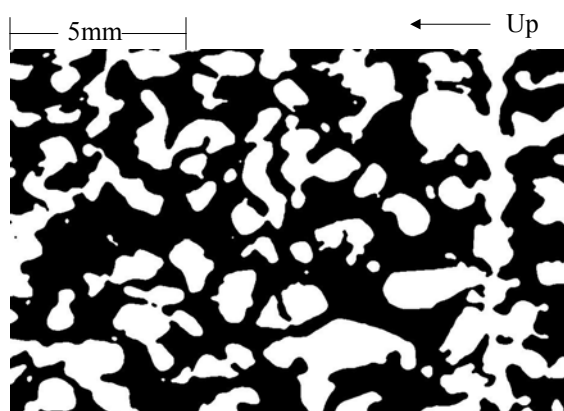


Figure 8. Ice layer from the 1999-1 firn core. Stratigraphic up is to the left.

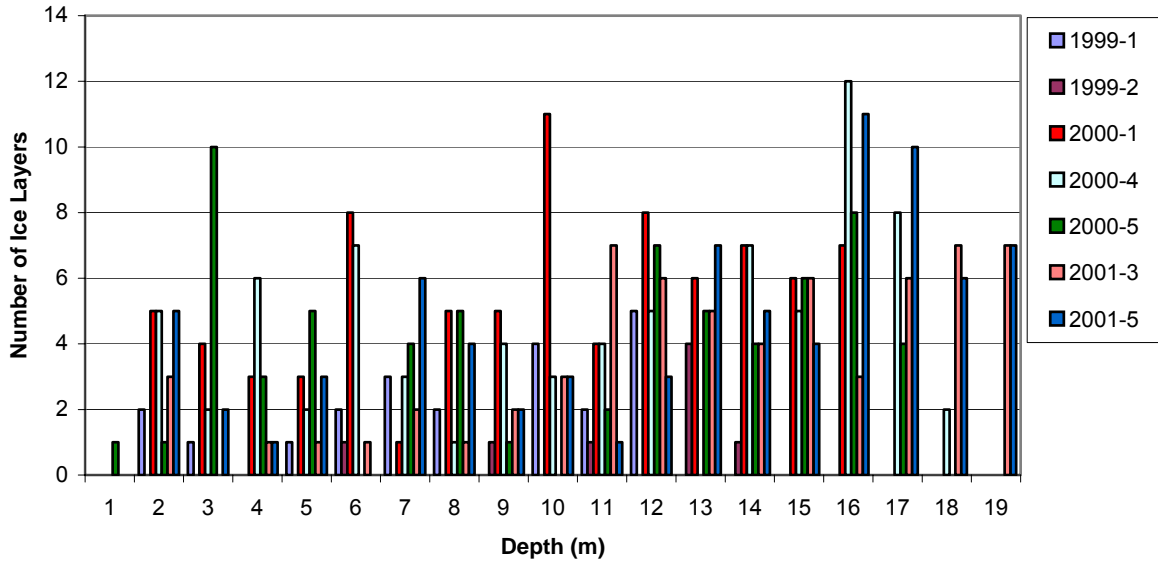


Figure 9. Frequency and distribution of single-grained ice layers throughout the ITASE firn cores.

Density and Porosity

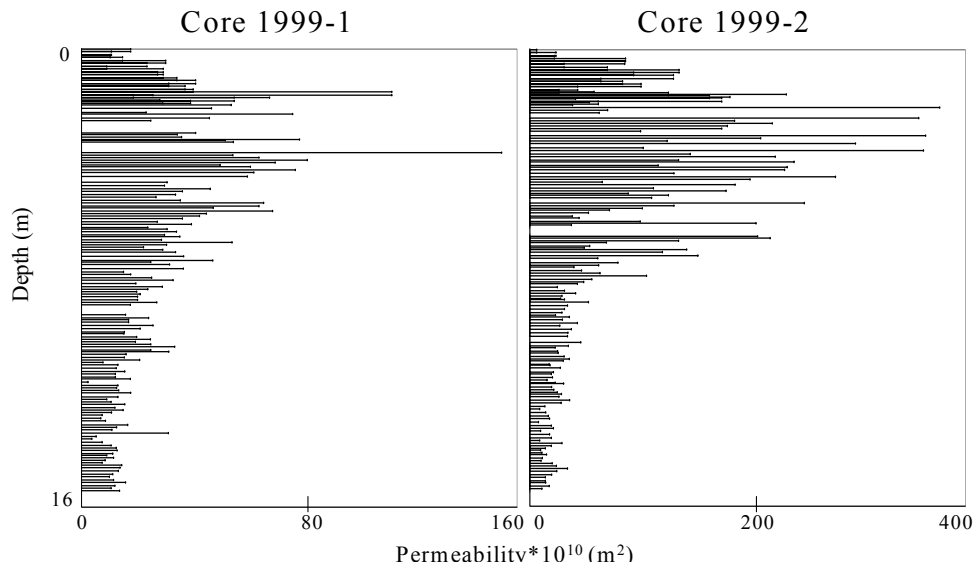
The density and porosity of each firn core were calculated, but the results are not included in this report. The porosity of each 10-cm section was needed for developing relationships to predict permeability, which could then be compared to measured permeability. Porosity was calculated using the density of the snow sample and the density of ice, which is 917 kg/m^3 :

$$p = 1 - \frac{\rho_s}{\rho_i} \quad (10)$$

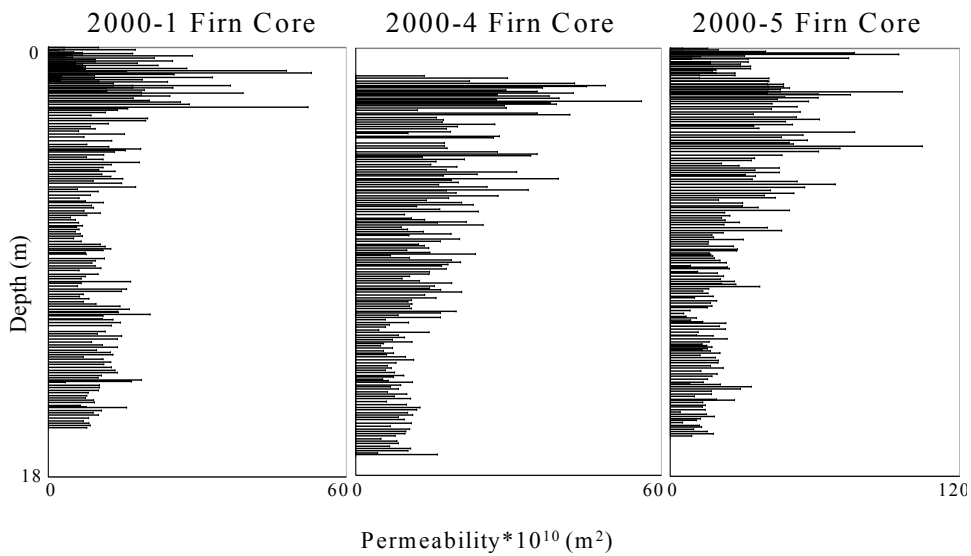
where the subscripts indicate snow or ice and p is porosity. As density increases with depth, the porosity decreases with depth. The change in density and porosity is due to the steadily increasing pressure in the firn core. As layers become buried, the snow above presses down, decreasing the amount of air space and increasing the snow density.

Permeability

Permeability profiles of each firn core are plotted in Figures 10a–c. There are no permeability data for the top meter of the 2000-4 core because the ITASE field team did not measure permeability from a snow pit at this site and the firn core began at a depth of approximately 1 m. As can be seen from the plots, the

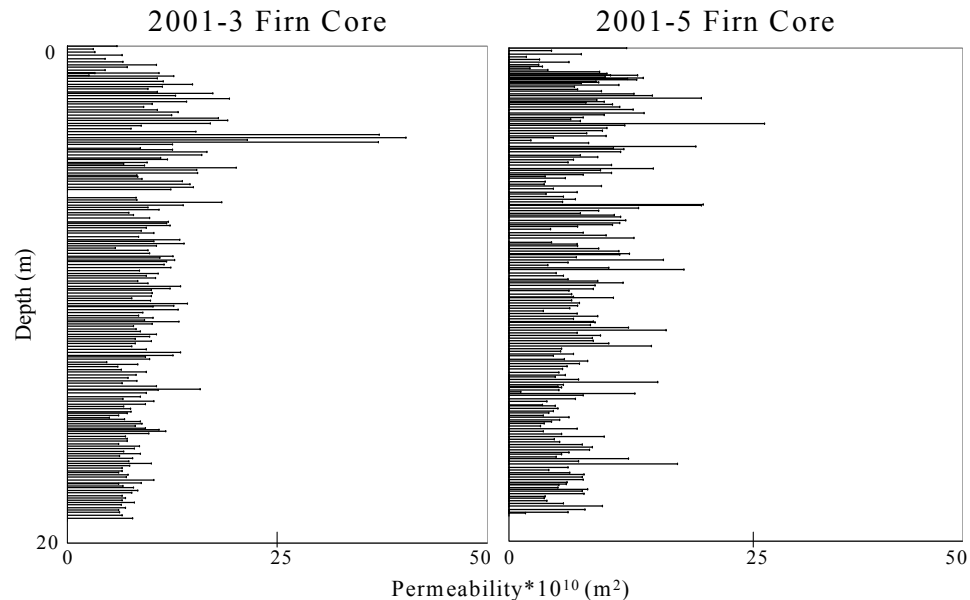


a. 1999 cores.



b. 2000 cores.

Figure 10. Permeability of the ITASE firn cores from 1999, 2000, and 2001. Permeability scales differ in order to show the shapes of the permeability profiles.



c. 2001 cores.

Figure 10 (cont.).

permeability varied greatly with depth in most cores and from site to site. Cores 3 and 5 from the year 2001 did not experience large permeability fluctuations with depth, and their overall permeabilities were very low relative to the rest of the ITASE firn cores. This suggests little metamorphism within the snowpack after deposition. On the other end of the permeability range, we find the 1999-2 firn core. This core has by far the highest overall permeability and also a great fluctuation in permeability with depth. This suggests a high rate of metamorphism, which was expected because of the site's low elevation, which results in higher mean annual temperatures. The remaining cores varied in permeability between the 1999-2 and 2001 firn core values.

Each of the firn cores exhibits a maximum permeability around 2–4 m (Fig. 10a–c). Beyond this depth the permeability gradually decreases in the 1999-1, 1999-2, 2001-3, and 2001-5 cores. The cores from 2000 also show a decrease in permeability with depth after 2–3 m, but they also show a second or third maximum in permeability. These deeper maxima are never of as great an amplitude as the one located at 2–3 m depth. It does not appear that these maxima or minima correspond to areas of decreased or increased ice layers. The frequency of the ice layers in each meter of each core was plotted (Fig. 9). Depths with high ice frequencies do not correspond to permeability minima in the 2000 firn cores. There must be another explanation for the permeability maxima in the 2000 firn cores; this will be discussed in the following chapter.

Microstructure

Quantitative microscopy and statistical measurements were made on several sections from each ITASE firn core. The data are extensive and not reported here but are available from the authors. The samples chosen for the comparison of firn cores were all homogeneous and fine in microstructure and were generally from the same depth or of a similar age as samples from other cores. Note that these homogeneous firn samples do not all have the same depth or age in each of the cores.

Grain Size

The actual statistic measuring grain size by IPW is the mean object intercept length. “Objects” in these images are snow grains, so it is the mean snow intercept length. This is the average length of the snow grains that intercept a test line across the image, so it is similar to a mean diameter of the snow grains. Robert Davis of CRREL has made comparisons between grain size measurements made with a hand lens and grain size calculated by quantitative microscopy. Groups of 40 people examined snow grains using hand lenses. The long and short axis lengths were used to calculate the cross-sectional area of each grain. Special care was taken to measure all sizes of snow grains in each snow sample because the human eye is naturally drawn to the larger grains. It was found that the quantitative microscopy measurements usually fell within one standard deviation of the mean of the hand lens measurements.*

Figure 11 shows that the grain size generally increased with depth in all of the firn cores. The grains were growing as a result of recrystallization. Near the surface, temperature gradient (TG) metamorphism caused the grains to grow rapidly. As the temperature gradients became larger, the grains grew faster. Deeper in the firn, where temperature gradients are not strong enough to drive TG metamorphism, the grains still grew as a result of equitemperature (ET) metamorphism. Overall, core 1999-2 had the largest grains, while the cores from 2001 had the smallest grains. The mean grain sizes reported here were calculated by the image processing software.

Gow (1969) visually measured grain areas of 0.24–0.68 mm² at South Pole from the surface down to 10 m, respectively. The South Pole measurements are areas, whereas the ITASE grain size measurements are lengths. Also, the average grain cross-sectional areas in the South Pole study were calculated from the average of the 50 largest grains in the sample because the samples were thin sections. When making a thin section, the grains are rarely cut at their widest part, so the average of every grain would underestimate the real grain size. A cross-sectional

* Personal communication, Robert Davis, CRREL, 2003.

area of 0.24 mm^2 corresponds to a diameter of 0.5 mm , which is similar to the mean intercept lengths near the surface in Figure 11.

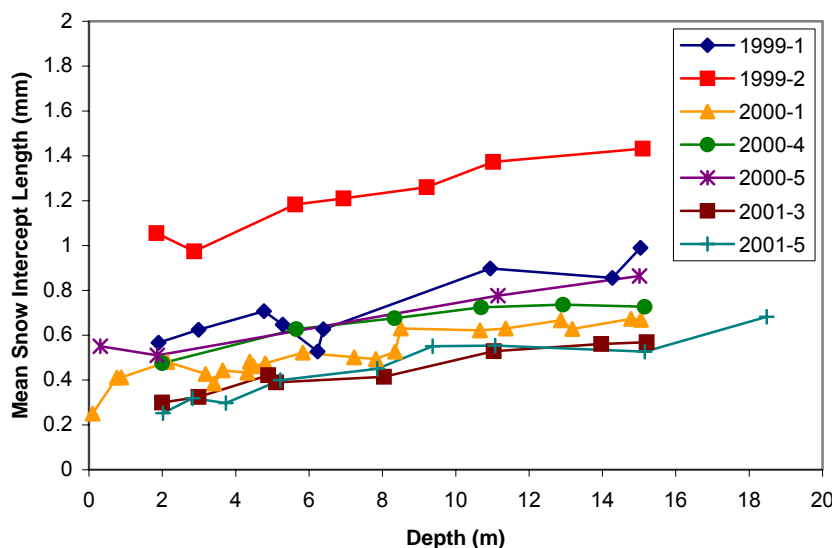


Figure 11. Mean snow grain size increase with depth of the ITASE firn cores.

Pore Characteristics

Pore size and shape are also important characteristics of the snow microstructure. Pore size is calculated in the same way as grain size. The mean pore intercept length is the average length of pore that intercepts a test line across the image. It can be seen in Figure 12 that pore size very gradually decreases with depth in cores 1999-1, 2000-4, 2001-3, and 2001-5. The firn core from 1999-2 has a more rapid decrease in pore size in the first 7 m (Fig. 12). The mean pore size in the 2000-1 core increases to a depth of about 1.5 m and then decreases. This pattern is not evident in the other cores, either because it did not occur there or because not enough samples were analyzed to reveal the pattern. The increase in pore space very near the surface in the 2000-1 core is probably caused by TG metamorphism, which destroys the necks between grains and causes the growing grains to push away from each other. The competing mechanism that causes the pores to become smaller is the overburden pressure. As the snow becomes buried, the pressure on it continually grows, so the pores are gradually squeezed smaller with increasing depth. The importance of the overburden pressure will be discussed in the next chapter. At depths without temperature gradients, the snow begins to sinter together, creating necks between snow grains and closing off pores.

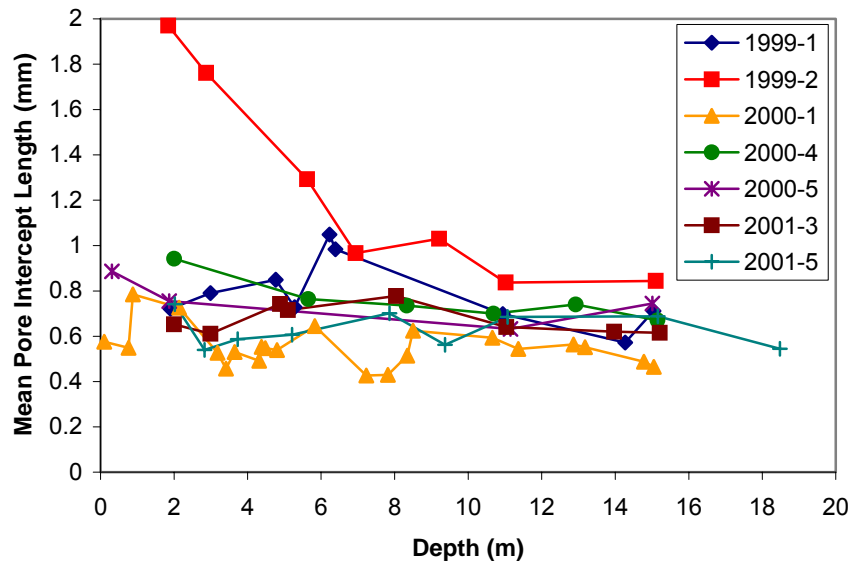


Figure 12. Mean pore size with depth of the ITASE firn cores.

Grain Characteristics

Surface density and specific surface are measures of the amount of surface area of snow there is based on total volume and volume of snow, respectively. Overall, the surface density of the 1999-2 core is the lowest (Fig. 13), suggesting

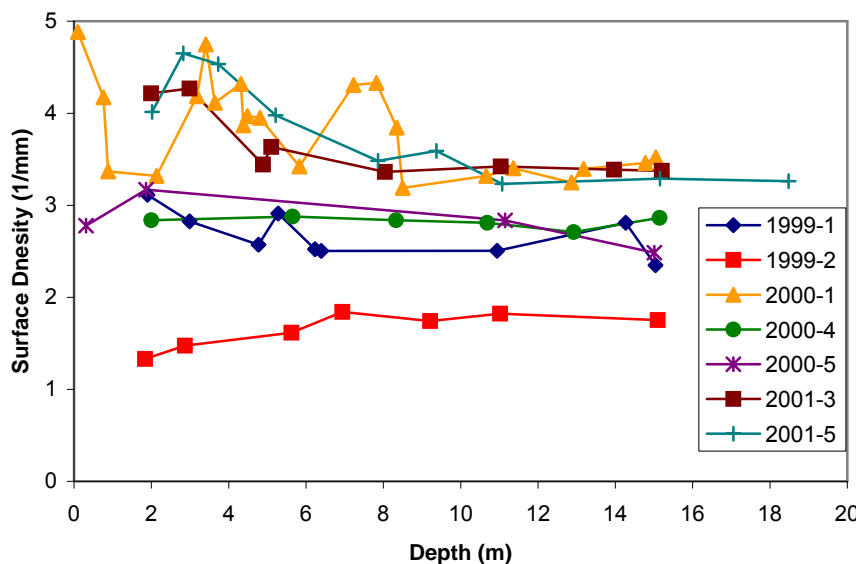


Figure 13. Surface density of the ITASE firn cores.

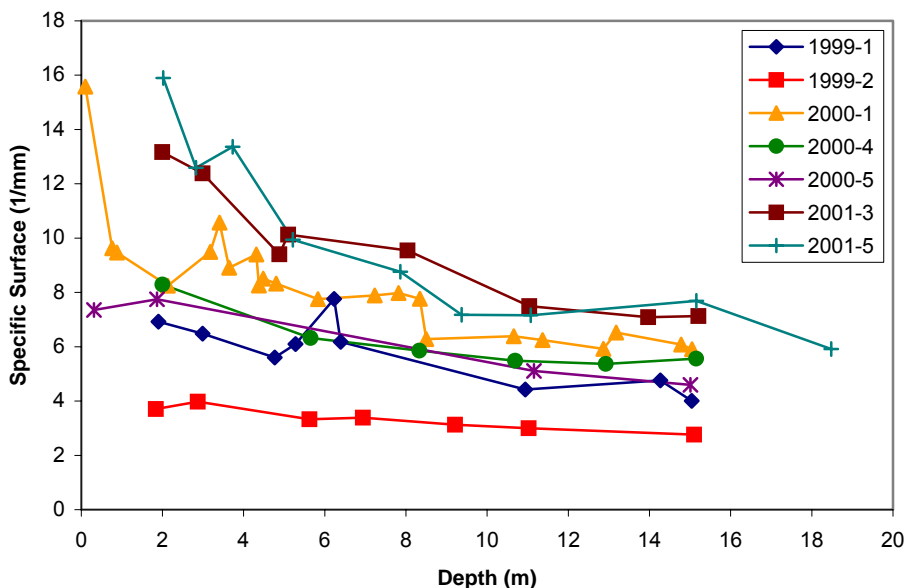


Figure 14. Specific surface of the ITASE firn cores.

fewer large grains rather than many small grains. This decrease in surface is a result of the recrystallization processes, which drives the snow grains to reduce the amount of surface energy they have. With depth the surface density is relatively steady; however, the specific surface decreases with depth in all ITASE firn cores (Fig. 13 and 14).

Waddington et al. (1996) found the specific surface area of polar firn to be $0.0375 \text{ m}^2/\text{g}$ by assuming that the firn was composed of many closely packed spheres and solving analytically. Hoff et al. (1998) found the specific surface area of seasonal snow to be between 0.12 and $0.37 \text{ m}^2/\text{g}$ by nitrogen gas adsorption experiments. Cabanes et al. (2002) found the surface area of 10-day-old polar snow to be $\sim 0.0300 \text{ m}^2/\text{g}$ by CH_4 adsorption. The quantitative microscopy measurements of specific surface are with respect to the volume of the sample or snow and not the mass. Converting the quantitative microscopy measurements into per-mass values, we find that a $400\text{-kg}/\text{m}^3$ -density sample with a 10-mm^{-1} specific surface calculated by quantitative microscopy has a specific surface of $0.025 \text{ m}^2/\text{g}$ by mass. The Hoff et al. (1998) study used fresh seasonal snow, which is dendritic and has much greater surface area than aged firn, which may explain why their specific surface values are much greater than those for polar firn.

Detailed Microstructure Characteristics of One Site

Because of time constraints it was not possible to analyze every section of every ITASE firn core. Thus, for this report, one core was chosen on which to concentrate efforts at understanding microstructural metamorphism with time and the impact of aging. Core 2000-1 was chosen because of its geographic location near the proposed site for the Inland WAIS Deep Core project and its midrange permeability profile relative to the other cores. Site 2000-1 is of particular importance to the ice coring community because it will be important to understand snow microstructure characteristics at this site for chemical modeling in support of the deep ice core interpretation.

All homogeneous core sections in the 2000-1 firn core were analyzed. The permeabilities of approximately 10-cm sections throughout the entire length of the core were measured. As can be seen by Figure 10b, the permeability increased gradually to a maximum at about 2 m and then gradually decreased. Figure 15 shows the permeability profile with age. The first maximum corresponds to an age of about 2.5 years. There is another maximum of lesser amplitude around 12 m, or 35 years. Possible explanations for this second maximum will be discussed in the next chapter.

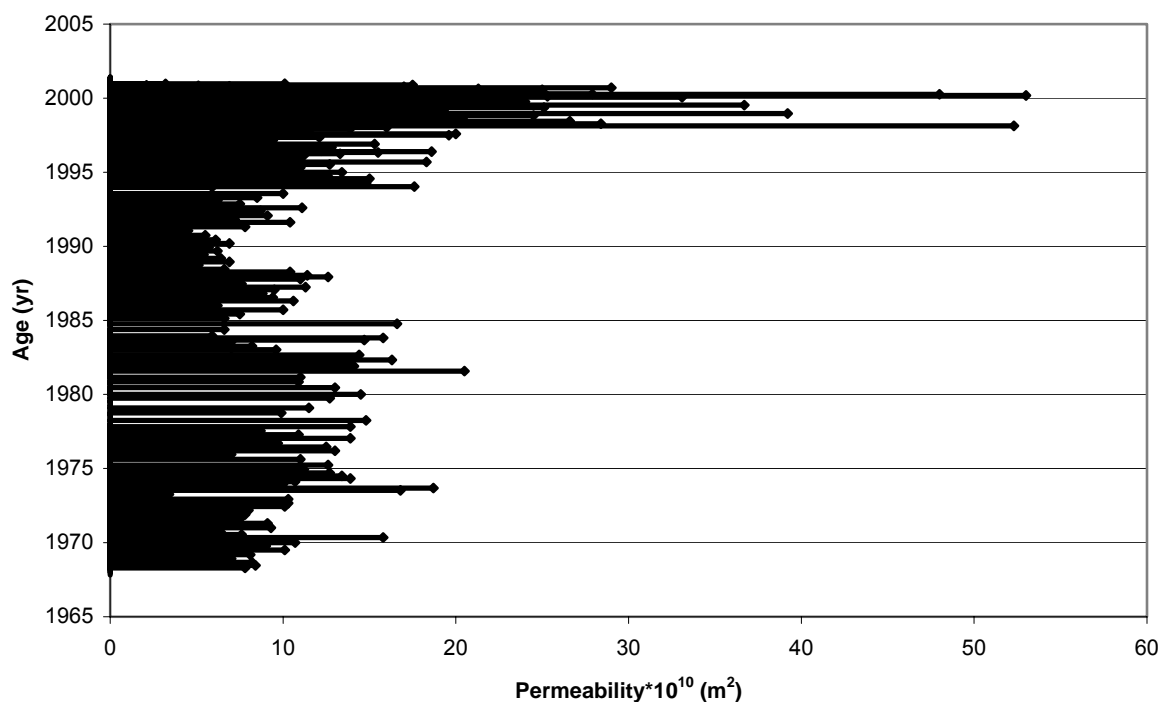


Figure 15. Permeability profile of 2000-1 core with age. Dan Dixon of the University of Maine provided the depth–age scale required to make this plot.

The quantitative microscopy measurements are plotted in Figures 16–20. Error bars have been included in each figure because quantitative microscopy measurements were made in two directions on each image, vertically and horizontally. The error bars represent the percent difference between the two measurements. The mean snow intercept length, or grain size, increases with depth, which is to be expected because of recrystallization in the forms of TG and ET metamorphosis (Fig. 16). The oscillation of the grain size and other stereological parameters occurs because both coarse- and fine-grained samples are included on the same plot. If only the fine-grained samples are plotted, one can better see the increase of grain size with depth (Fig. 17). Coarser-grained samples do not show such a smooth pattern because of the irregularity of the formation of such layers, although they do still indicate an increase in grain size with depth (Fig. 18 and 19). Some coarse layers are depth hoar and have very large grains and pores, while others are sugar snow and have large grains but smaller pores.

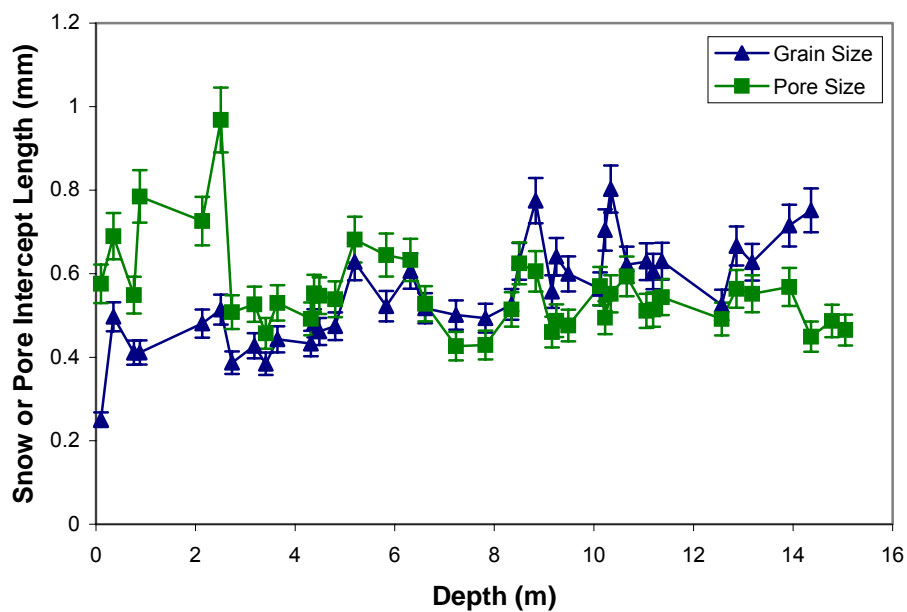


Figure 16. Mean grain and pore intercept lengths of the homogeneous 2000-1 firn core samples.

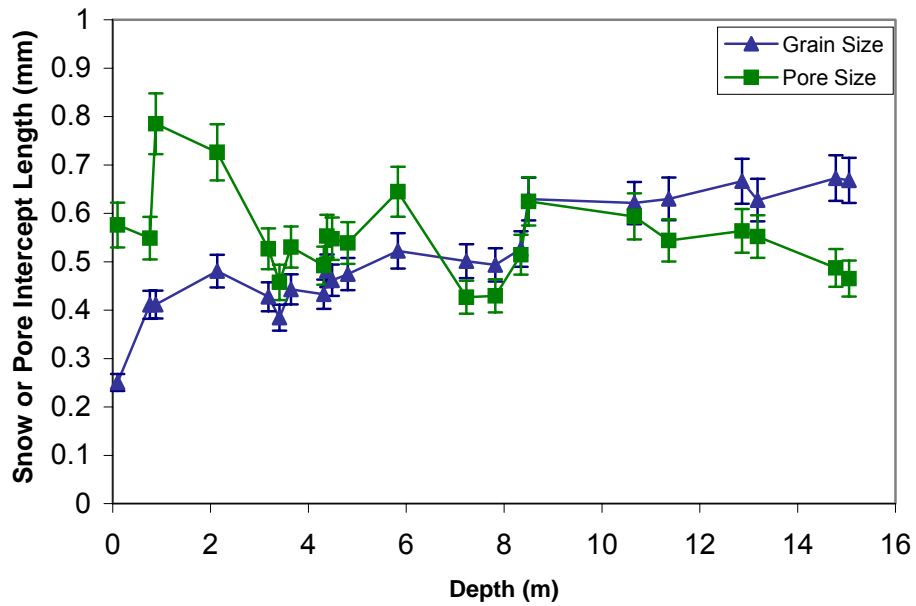


Figure 17. Mean grain and pore intercept lengths of the fine-grained 2000-1 samples only. This plot better illustrates grain growth, as only samples of similar snow type are included.

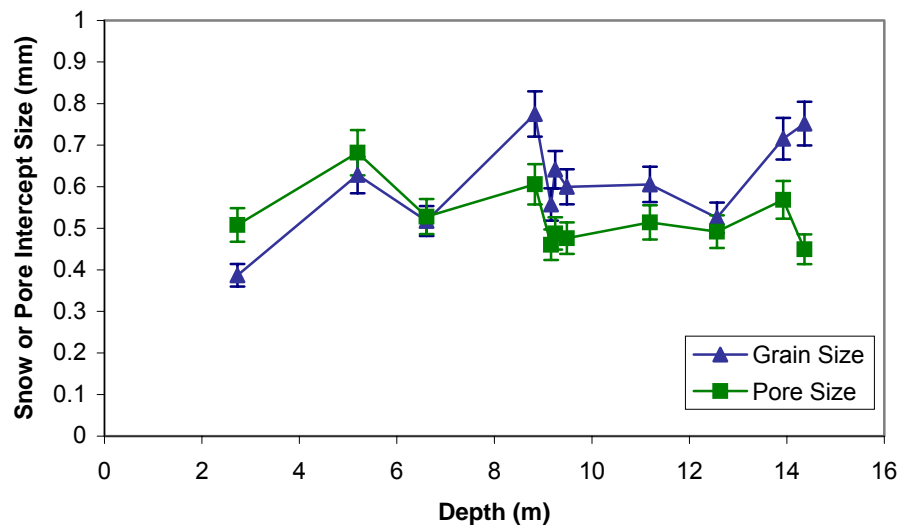


Figure 18. Coarse/fine-grained sample of 2000-1 firn core. Grain size appears to be increasing but irregularly.

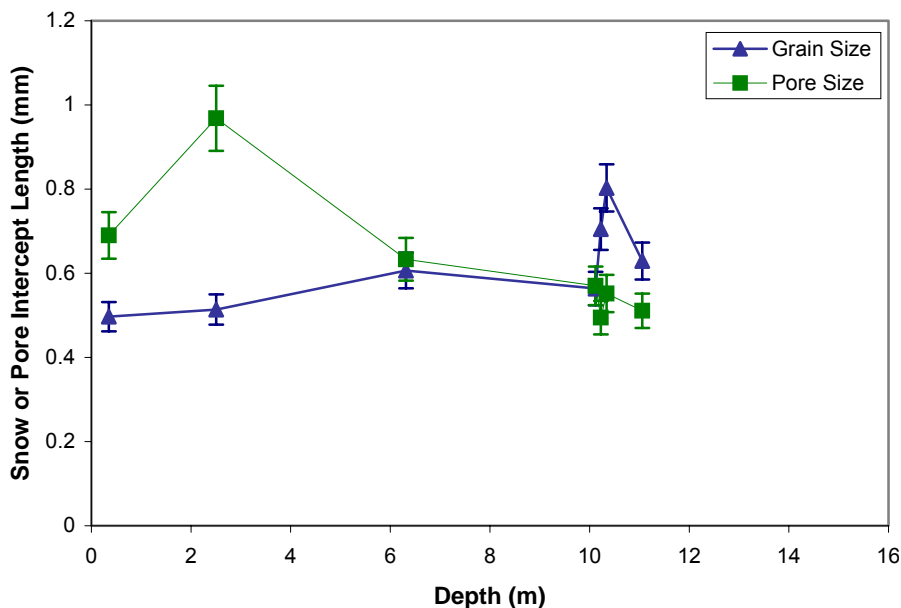


Figure 19. Mean grain and pore size of coarse-grained 2000-1 samples.

From Figure 17 we see that the pore size increases to a depth of 2.5 m and then decreases. It is important to note that this pattern is different than for the grain size. While grain size continuously increases down through the core, pore size increases and then decreases as in the permeability profiles. This similarity prompted further investigation, which is discussed in greater detail in the next chapter.

The surface density of the snow, which is the amount of snow surface area with respect to the entire sample volume, did not have an apparent pattern with depth. It can be seen in Figure 20 that the specific surface, however, does show more of a correlation with depth. The specific surface gradually decreased with depth. This is also due to thermodynamic processes driving the snow grains to decrease their surface energy. ET metamorphosis causes the snow grains to round and large grains to grow at the expense of small grains. This also decreases the amount of surface. Specific surface is a more useful parameter because it takes into account the changing volume fraction of the snow. In the surface density measurement, no attention is paid to the amount of snow in the total volume. So while the surface density is changing, so is the volume fraction of snow.

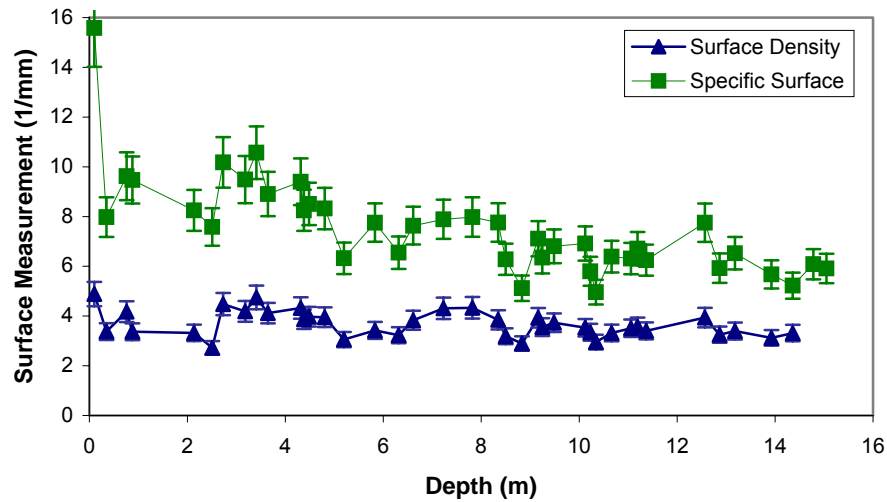


Figure 20. Snow surface measurements of the 2000-1 firn core.

There are several interesting patterns evident in the metamorphism of the snow grains in core 2000-1. These will be related to the permeability, site temperature, and accumulation rate along with those of the other ITASE cores. This will be done to gain a better understanding of why and how the snow changes after deposition and how these changes affect the permeability profiles within the snow and firn.

5 DISCUSSION

Temperature Gradients in the Firn

Before discussing microstructure changes in the firn, it is important to understand the temperature conditions in the firn. Temperature gradients determine what type of metamorphism the snow will undergo, and they are present in the firn because of temperature oscillations at the surface of the snow. For an analytical solution we assume that the firn temperature is controlled by diffusion; by assuming harmonic temperature oscillations at the surface, we can derive an exact solution. The temperature oscillations cause the temperature in the firn to vary in time and space according to Equation 11:

$$\frac{\partial(T - T_s)}{\partial t} = \alpha \frac{\partial^2(T - T_s)}{\partial x^2} \quad (11)$$

where α = thermal diffusivity of the firn
 T = temperature in the firn
 T_s = mean annual temperature
 t = time
 x = location in the firn.

Equation 10 can be solved by separation of variables and can be simplified by assuming that the surface oscillations are harmonic, as in Equation 12:

$$T - T_s = T_a \cos\left(\frac{2\pi t}{p}\right) \quad (12)$$

where T_a = amplitude of the temperature oscillation
 t = time
 p = period of the temperature oscillation.

Using this harmonic function with the solution to Equation 11, we get:

$$\frac{T - T_s}{T_a} = \exp\left[-2\pi\left(\frac{x}{2\sqrt{\pi p \alpha}}\right)\right] \cos 2\pi\left(\frac{t}{p} - \frac{x}{2\sqrt{\pi p \alpha}}\right). \quad (13)$$

Two important temperature oscillations are diurnal and seasonal, and it would be useful to know how deep into the firn these temperature oscillations are seen. We will assume that the temperature oscillation has disappeared if its amplitude at depth is less than 1% of its amplitude at the surface. Thus,

$$\exp\left(-2\pi\frac{x}{2\sqrt{\pi\rho\alpha}}\right) < 0.01. \quad (14)$$

This leads to Equation 15, which gives the depth at which the temperature oscillation at the surface can no longer be seen in the firn:

$$x = 0.73\left(2\sqrt{\pi\rho\alpha}\right). \quad (15)$$

Diurnal oscillations, with a period 24 hours, penetrate only approximately 15 cm into the firn. Seasonal oscillations, with a period 8760 hours, penetrate approximately 250 cm into the firn. These depths were calculated assuming homogeneous firn with a density of 400 kg/m³. In reality, firn is highly layered with varying density and thermal properties, so these depths are estimates. Data from an Antarctic site verify these depth calculations.

Firn temperature gradients were not measured at the ITASE sites; however, measurements were available from Siple Dome, Antarctica. This site is in West Antarctica, as are the ITASE firn core sites, so the temperature gradients in the firn may be similar. Siple Dome is nearer to the coast, however, so it does not have the same meteorological conditions as the ITASE sites; thus, its micro-structure and permeability will be different. The Siple Dome firn temperature was measured with a 23-thermocouple array situated from 55 cm above the surface down to 553 cm into the firn. The array was placed in the firn along with a datalogger in mid-November. The datalogger stopped recording near the end of June the following year. Every hour the datalogger would record the firn temperature at each thermocouple. The temperature gradient in the firn can be found by calculating the difference between firn temperatures and dividing by the distance between the thermocouples.

The magnitude of the temperature gradient will drive the rapid crystal growth near the surface. The sign of the temperature gradient determines the direction of heat flow and therefore crystal growth. For this discussion, we are only interested in the magnitude of the gradients so that we may find the degree of rapid crystal growth and the depths at which TG metamorphism occur. Figure 21 gives the magnitude of the temperature gradients with depth in the firn averaged over the

entire seven months that the datalogger was recording. The firn between the surface and 20 cm has a much steeper temperature gradient than the adjacent layers because of diurnal temperature oscillations. The temperature gradients between 20 and 100 cm are most likely caused by seasonal temperature oscillations.

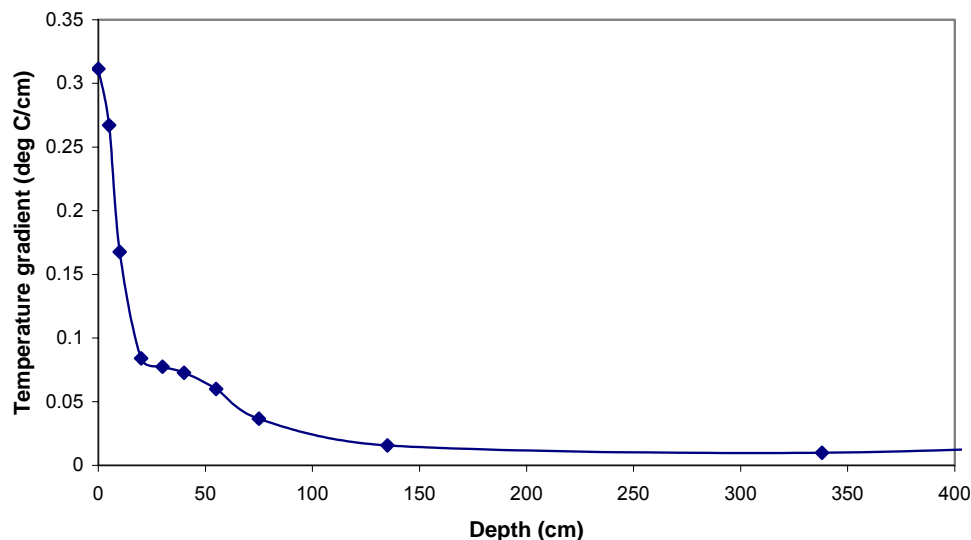


Figure 21. Magnitude of temperature gradients averaged over 7 months at Siple Dome.

Colbeck (1982) determined that a gradient of at least $0.1^{\circ}\text{C}/\text{cm}$ was required for rapid growth of large grains (TG metamorphism). If the ITASE firn cores have firn temperature characteristics similar to those of the Siple Dome site, TG metamorphism only occurs down to a depth of about 20 cm. Below 20 cm the temperature gradients gradually decrease with depth. Wherever the temperature gradients are not strong enough to drive TG metamorphism, ET metamorphism takes over. This will be important to understand in the following discussions of permeability/microstructure relationships.

Density Increase with Depth

Over a several-hundred-meter ice core, the density increases monotonically but not at a constant rate. Near the surface the firn density increases more rapidly, and there is a greater variation in density between layers. Gow (1968) found that the rate of densification slows at around 10 m in the Byrd ice core and the Little America V ice core, and he attributed this to changing densification mechanisms. These mechanisms were not explained in detail, however. The decrease in densification rate occurred at a shallower depth for the ITASE firn cores. Table 2 give

the ITASE firn core site temperatures, accumulation rates, depth of densification rate change, and densification rates, taken from the density–depth plots below, apparent in the firn cores.

Table 2. Mean annual temperature, accumulation rate, and densification information for ITASE firn cores. “Surface densification rate” refers to the rapid density increase with depth seen in the top few meters of the firn. “Deep densification rate” refers to the slower density increase with depth seen below approximately 3 m in the firn.					
ITASE firn core	Mean annual temp. (°C)	Accum. rate (H₂O equiv. in cm/yr)	Surface densification rate (kg/m³/m)	Deep densification rate (kg/m³/m)	Depth of change in densification (m)
1999-1	-25.4	14.7	19	11	6
1999-2	-21.5	13.4	30	14	6
2000-1	-29.5	17.2	27	8	4
2000-4	-29.0	17.3	32	10	4
2000-5	-29.7	11.9	16	12	4
2001-3	-25.9	33.9	16	8	6
2001-5	-26.4	36.4	20	8	6

Gow (1968) found that the rate of densification depends on the temperature and accumulation rate in the near-surface firn. As the temperature increases or the rate of accumulation decreases, the densification rate increases. The ITASE firn cores follow this pattern. The slopes of the density curves in Figures 22–24 show the rate of densification with depth. Cores 1999-2 and 2000-4 had the fastest density increase in the top 6 m, which is evidenced by their steep increase in density of about 30 kg/m³ per meter of depth in the core. The 1999-2 core also has the greatest rate of densification below 6 m. The 1999-2 site had the highest mean annual temperature and the second lowest accumulation rate, and the corresponding ITASE ice core had an extremely shallow firn–ice transition depth of 36 m,* all evidence of rapid densification.

Conversely the 2001 cores had very high accumulation rates and more moderate temperatures than 1999-2. The 1999-1 and 2000 firn cores had moderate accumulation rates but low annual temperatures. These combined effects result in similar densification rates for all of the firn cores other than 1999-2. The 2001 cores’ very high accumulation rate would likely have resulted in very slow densification, but the moderate temperature counteracted this effect. Similarly, the low

* Personal communication with Dr. Anthony Gow, CRREL, 2002.

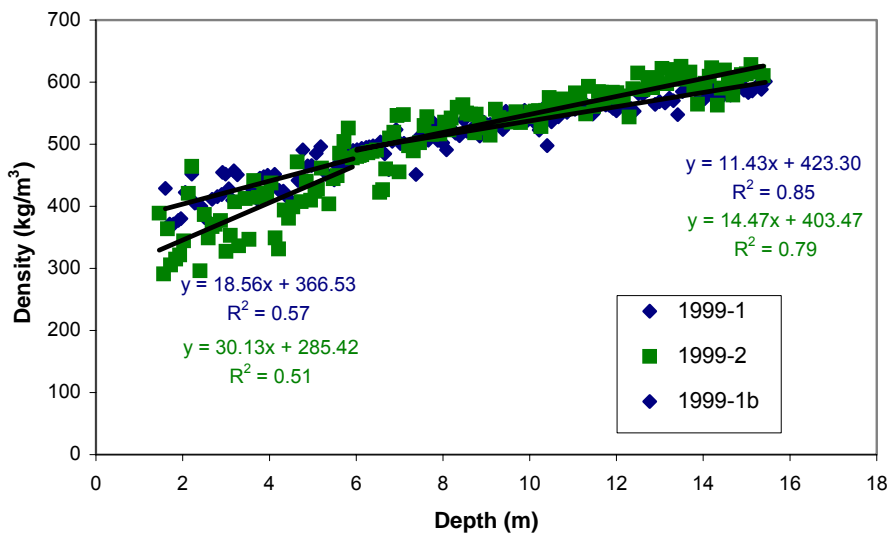


Figure 22. Density increase with depth of the ITASE 1999 firn cores. The change in slope or rate of densification occurs at around 6 m in both firn cores.

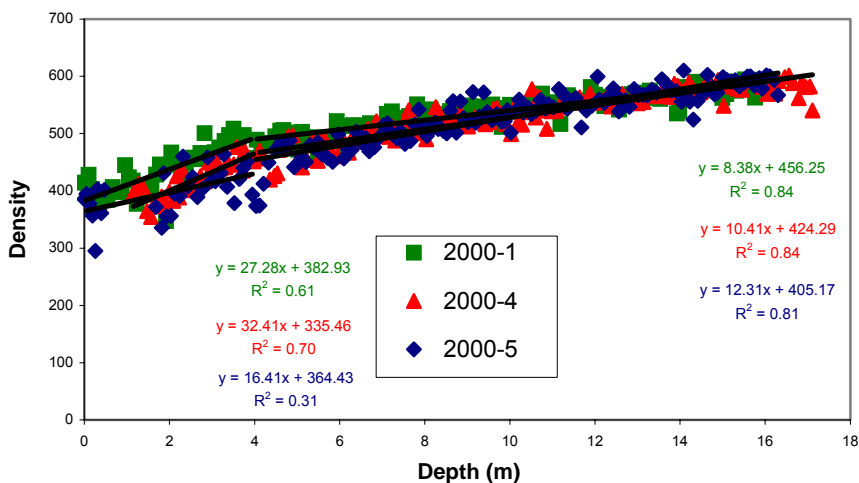


Figure 23. Density increase with depth of the ITASE 2000 firn cores. The change in slope or rate of densification occurs near 4 m in all three firn cores.

temperatures of the 2000 firn cores would likely have resulted in low densification rates, but it is the low accumulation rates that counteracted this effect.

The greatest variation in density from layer to layer occurs near the surface, while there is less variation in the deepest parts of the firn cores. Thus, there is

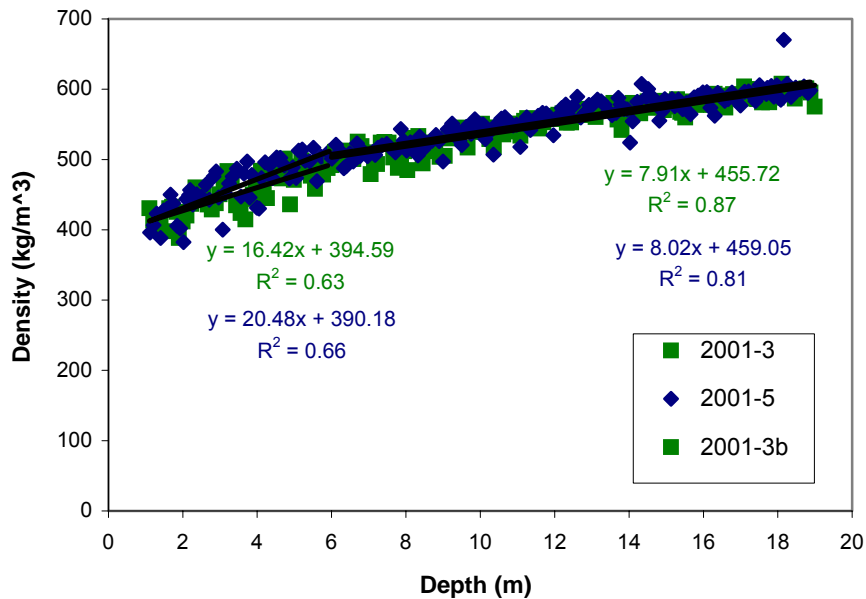


Figure 24. Density increase with depth of the ITASE 2001 firn cores. The change in slope or rate of densification occurs at around 6 m of both firn cores.

poor correlation of the near-surface trend lines in Figures 22–24. This high degree of variation is due to the variation in crystal structure. The coarse-grained layers tend to have lower densities than the fine-grained layers. Near the top of the core, the wind pack layers are very different in microstructure from the hoar layers. These large variations in grain structure are less pronounced after metamorphism has taken place for several years, thus smoothing out the density profiles. The 1999-2 core has the greatest density variation within the top 6 m, and it also has the greatest degree of metamorphism. In contrast, cores 2001-3 and 2001-5 have much less density variation and also very little metamorphosis.

Density is affected by the firn microstructure as is permeability, but density is a poor predictor of permeability. The densities of the ITASE firn cores are similar, while the permeability profiles are very different from site to site. Density constantly increases with depth at all of the ITASE sites, but the permeability does not. We have seen that the competing effects of temperature and accumulation rate can result in similar densities for sites of very different meteorological conditions. The permeability profile with depth takes on a different shape and is likely caused by the different meteorological conditions rather than the densification of the firn.

Changes in Permeability with Depth

Effects of Microstructure

The permeability profiles of the ITASE firn cores have an overall similar shape (Fig. 10a-c). The permeability increases to a maximum around 2–4 m for the firn cores. Then it decreases gradually with depth. This increase and decrease in permeability with depth can be explained by the firn microstructure and metamorphism.

The top ~3 m of firn are exposed to seasonal and diurnal temperature gradients, with the top ~20 cm experiencing temperature gradient (TG) metamorphism. Sufficiently strong temperature gradients are also responsible for the formation of depth hoar in the firn (Alley et al. 1990), which is an extreme case of TG metamorphism. Depth hoar layers are relatively thin but have very high permeability resulting from their large, elongated crystals and large pores. Below 20 cm ET metamorphism takes over in the firn. This type of metamorphism also results in grain growth, but at a slower rate than TG metamorphism. The firn between 20 cm and ~3 m experiences seasonal temperature gradients. Thus, the firn is warmer for half of the year, and the rate of ET metamorphism is accelerated. TG metamorphism produces increased pore space because of the sublimation of smaller grains (Fig. 25); thus, it produces more permeable layers because the pore network is opened up. With the progression of TG metamorphism, the firn becomes more and more permeable, resulting in an increase in permeability with depth very near the surface.

Inter-layer temperature gradients decrease with depth until the temperature gradients between layers are very small, resulting in equitemperature (ET) metamorphism, which is caused by surface energy reduction over snow grains. ET metamorphism leads to rounded, highly sintered snow grains, which reduces the permeability of the snow as necks form and close off the pore throats. In Figure 26 we can see that instead of a network of pores, there is now a network of grains. ET metamorphism is one mechanism responsible for the decrease in permeability deeper in the firn cores.

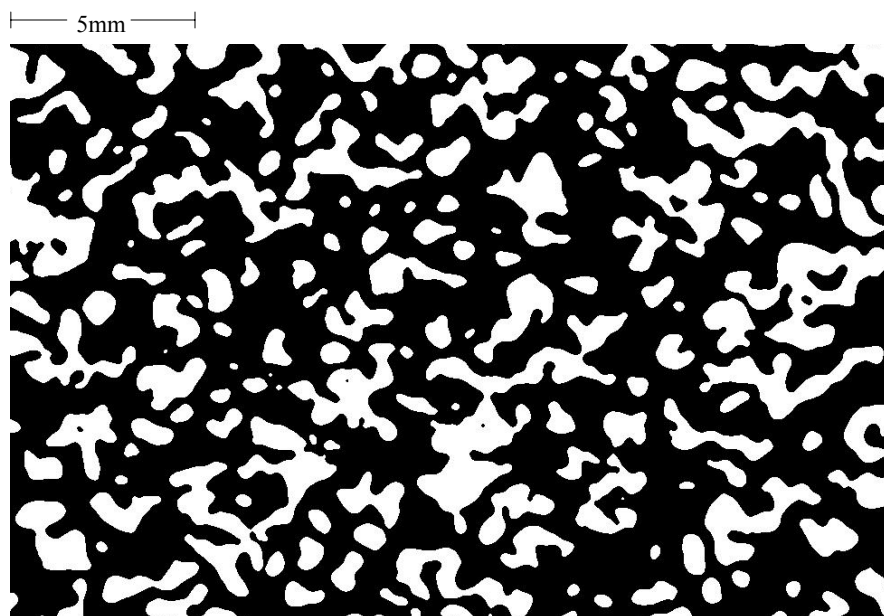


Figure 25. Coarse-grained sample of the 2000-1 firn core at a depth of 2.5 m. Stratigraphic up is to the left. Note that not all of the smaller grains have been removed by metamorphism.

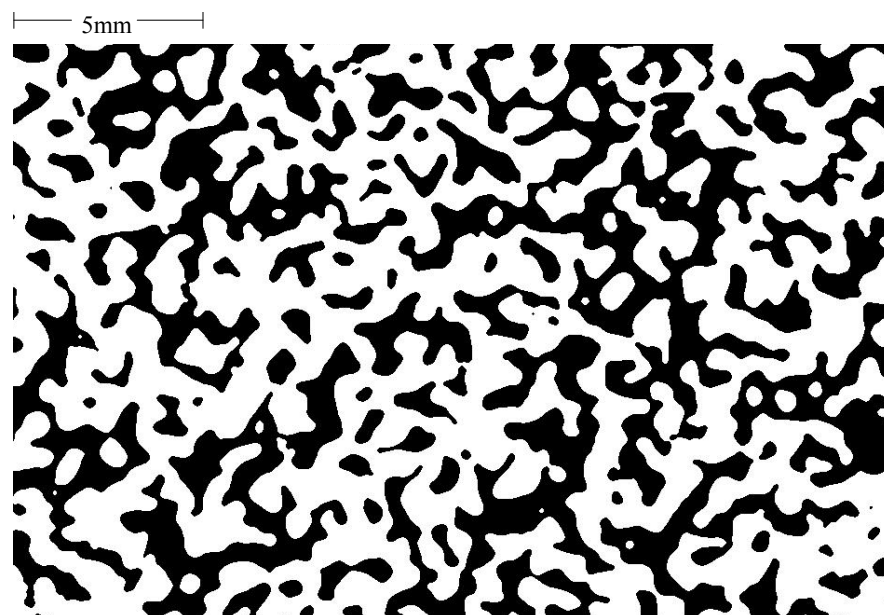


Figure 26. Fine-grained sample of the 2000-1 firn core from a depth of 10.34 m.

Effects of Overburden Pressure

The overburden pressure is another possible mechanism affecting the permeability. At the maximum compression strength of the snow, the necks between snow grains begin to fail. If the overburden pressure exceeds the compression strength of firn, the compression stress begins to press the snow grains together, gradually decreasing the pore space and interconnectedness of the pore network. Thus, the permeability would also decrease. We must determine the stress conditions in the firn.

Figure 27 shows the increase in compression stress due to overburden pressure with depth in the ITASE cores. The overburden pressure throughout each firn core was calculated using the mass of each core section. By summing the total mass of snow over a desired depth and multiplying by gravity, the total force at that depth can be calculated:

$$F = mg \quad (16)$$

where g = gravity
 m = total mass of the column of snow
 F = force.

This force can be used to find the compression stress at any point in the firn core:

$$\sigma = \frac{F}{A} \quad (17)$$

where σ is the compression stress in MPa and A is the cross-sectional area of the column of snow. Figure 27 shows that the compression stress increases nearly linearly with depth. The actual curve of best fit is a very shallow parabola. The rate of pressure increase varies very little from core to core (Fig. 27). The overburden pressure in the 1999-2 core does not increase as rapidly with depth near the surface, but “catches up” deeper in the firn. Even though the 1999-2 core had one of the highest densification rates, its surface snow started out at a much lower density (Fig. 22), so the overburden pressure near the surface was not as high as the other firn cores. The density at greater depths in this core became the same as the other cores because the 1999-2 core was increasing in density at a faster rate (Fig. 22).

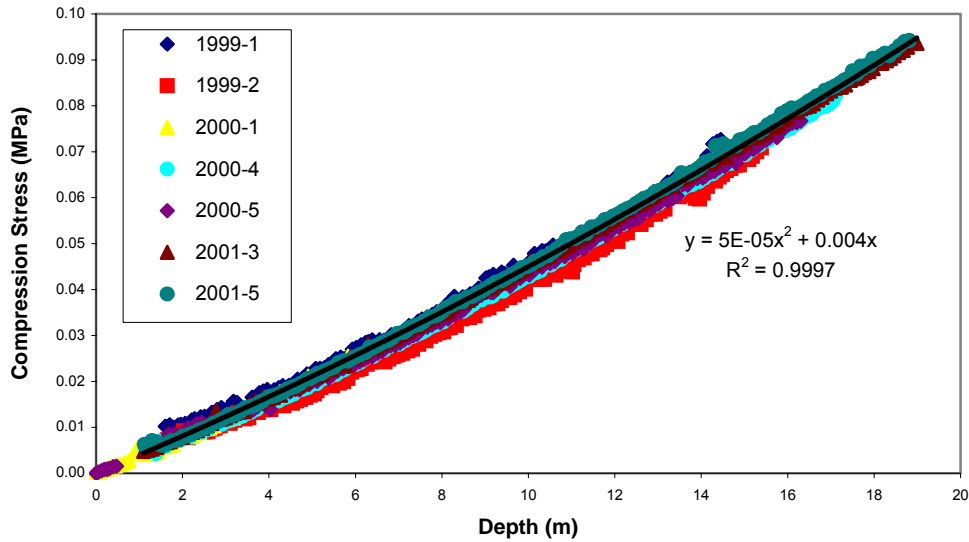


Figure 27. Compression stress increase throughout each firn core. Compression stress was calculated using the summed masses of the core sections.

Compression strength has been found to increase with the density of snow (Mellor 1975, Abele and Gow 1975). Abele and Gow (1975) plotted the unconfined compressive strength range with density of natural firn. Generally the ITASE firn cores ranged in density from about 350 kg/m³ near the surface to 600 kg/m³ at a depth of 15 m. Table 3 gives the lower and upper limits of the range of compression strengths [from Abele and Gow (1975) plot] at various densities found in the ITASE firn cores.

Density (kg/m ³)	Lower limit of compression strength (MPa)	Upper limit of compression strength (MPa)
350	0.055	0.090
400	0.069	0.27
450	0.27	0.55
500	0.62	0.93
550	1.1	1.5
600	1.6	2.1

We would like to know at what depth the snow begins to fail due to compression stress. The trouble lies in knowing the compression strength of polar firn. Different snow types have different compression strengths. In general, fine-grained layers such as wind pack are stronger than coarse-grained depth hoar. Depth hoar grows at such a rapid rate that the grains have no time to sinter together, creating a weak layer (Colbeck 1982). Abele and Gow (1975) did not specify which type of grains the compression strengths pertain to. Also, the lowest density recorded by Abele (1990) was 350 kg/m^3 . A few of the ITASE firn cores had lower-density samples near the surface.

Table 4 shows the greatest overburden pressures reached near the bottom of the ITASE firn cores. These stresses would cause failure in snow with a density of about 400 kg/m^3 according to Abele and Gow (1975), but the density at the core bottoms is much higher, so the strength should be much higher. By comparing the density and overburden pressures throughout each ITASE firn core to the plot in Abele and Gow (1975), we found that the compression strength is not exceeded in these firn cores. However, density is an incomplete predictor of compression strength because the strength of the snow depends on how many snow grains are sintered together. The amount of sintering depends on the type of snow.

ITASE firn core	Depth at core bottom (m)	Overburden pressure at bottom (MPa)	Maximum density near core bottom (kg/m^3)
1999-1	15.430	0.075	601
1999-2	15.385	0.071	628
2000-1	15.930	0.077	594
2000-4	17.110	0.082	602
2000-5	16.305	0.077	610
2001-3	18.991	0.094	608
2001-5	18.814	0.094	670

No mechanical properties for specific types of polar snow (e.g. wind pack, depth hoar, etc.) were found in the literature. However, compression strength measurements have been made of surface snow near McMurdo Station on the Ross Ice Shelf in West Antarctica by Sally Shoop and Gary Phetteplace. They measured the compression strength of the top 2 m of firn using a cone penetrometer and found the strength of the firn to range from 0.08 to 0.4 MPa. This

range of compression strengths likely includes weak hoar layers and stronger wind pack layers. The highest stress seen by the ITASE firn cores between the surface and 2 m was 0.01 MPa. Clearly the overburden stress never reaches the compression strength of the firn in the top 2 m, so the firn layers are not failing near the surface. It also appears from the Abele and Gow (1975) data that the deeper firn layers in the cores we received were not failing either.

Temporal Changes in Microstructure

Core 2000-1 was used to study temporal variations in microstructure, so quantitative microscopy was completed on all homogeneous firn core sections. Figures 16–20 show the mean grain and mean pore intercept lengths and the surface measurements of the snow grains in core 2000-1. The mean grain intercept length, which is a measurement of grain size, shows a trend of increasing grain size with depth (Fig. 11). This is consistent with what is expected during snow metamorphism. Temperature gradients near the surface will cause grains to grow rapidly by TG metamorphism, while ET metamorphism will cause the grains to grow slowly below a depth of several centimeters. Figure 28 shows three images of fine-grained layers at three depths; one is near the surface, the second is near the permeability maximum, and the last is well below the permeability maximum depth where the permeability is smaller. Table 5 gives the information for each

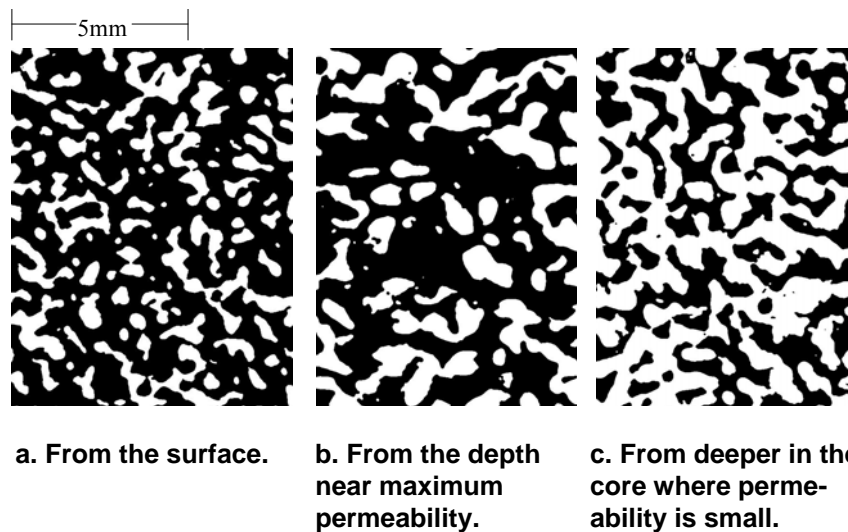


Figure 28. Three quantitative microscopy images from fine-grained layers in the 2000-1 firn core. The scale pertains to all three images, and stratigraphic up is to the left. Measured properties are given in Table 5.

Table 5. Microstructure and transport properties of three fine 2000-1 firn core samples pictures in Figure 28.

	a	b	c
Depth (m)	0.01	0.88	7.23
Density (kg/m ³)	428	398	539
Permeability ×10 ¹⁰ (m ²)	17.5	27.9	5.5
Mean grain size (mm)	0.25	0.41	0.50
Mean pore size (mm)	0.58	0.79	0.43

image. Note that the surface sample has smaller grains and more pore space, but the space is tortuous. The middle image has large grains and large, interconnected pores. The last image has smaller pores and the snow grains are now interconnected instead of the pores. This type of progression was found in all of the firn cores.

Figure 29 shows the mean snow grain intercept length, or grain size, as a function of time. The slope of this plot below 10 m is the isothermal linear growth rate of the crystals. Below 10 m the temperature gradients in the firn are very small and the growth rate is linear with time. Figure 29 shows that the isothermal growth rate of the firn below 10 m at the 2000-1 site was 0.0039 mm/yr with a firn temperature of -29.5°C . This is in good agreement with the results gathered by Gow (1969).

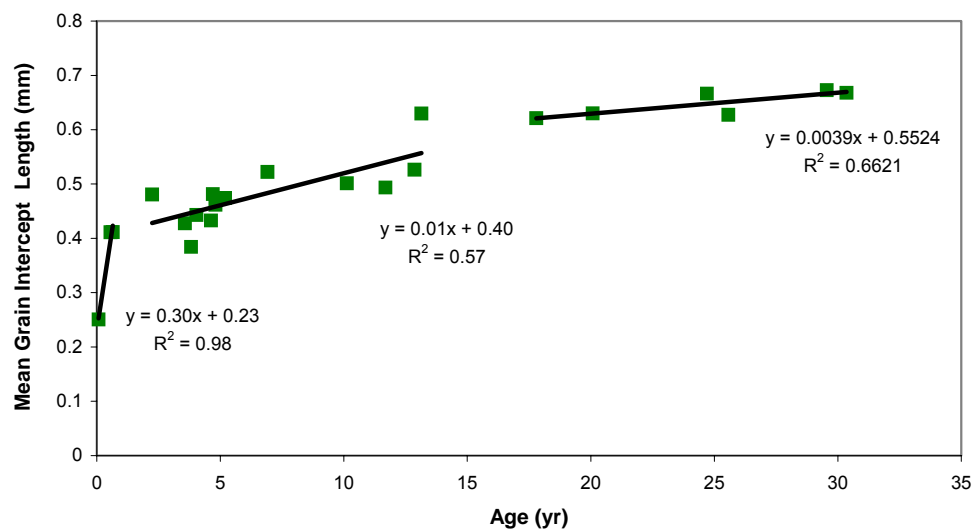


Figure 29. Growth rate of fine snow grains in the 2000-1 firn core. The linear growth rate below 10 m is 0.0039 mm/yr with a firn temperature of -29.5°C

Near the surface, the growth rate is neither isothermal nor linear with time. Temperature gradients drive crystal growth in the near surface, and the gradients may vary seasonally or diurnally. When the gradients are large, as they are in the top 20 cm, the grain growth is rapid. Between 20 cm and 10 m, the temperature gradients are too weak to drive TG metamorphism, but ET metamorphism occurs at a faster rate than below 10 m because the firn is experiencing seasonal temperature oscillations and is warmer for half of the year (Fig. 21). These three rates of grain growth in the 2000-1 firn core are apparent in Figure 29. The very rapid grain growth in the top meter is caused by the strong temperature gradients at the firn surface caused by daily fluctuations in the firn temperature. The middle area of grain growth between the top meter and 10 m has moderate temperature gradients, which are a result of seasonal temperature variations, that are too weak for TG metamorphism, so ET metamorphism takes over. The deepest area of grain growth is where very small temperature gradients occur, as mentioned above.

Other microscopic parameters that change with time are specific surface and pore size. Figure 30 shows the decrease in specific surface with time. The surface is decreasing because large grains are growing at the expense of smaller grains, and the grains are becoming more rounded. Many sharp angles on a grain mean that it has a high surface area, while a more rounded grain has less surface. Also, many small grains would have more total surface area than fewer, larger grains. Figure 30 shows a very rapid decrease in specific surface at the surface of

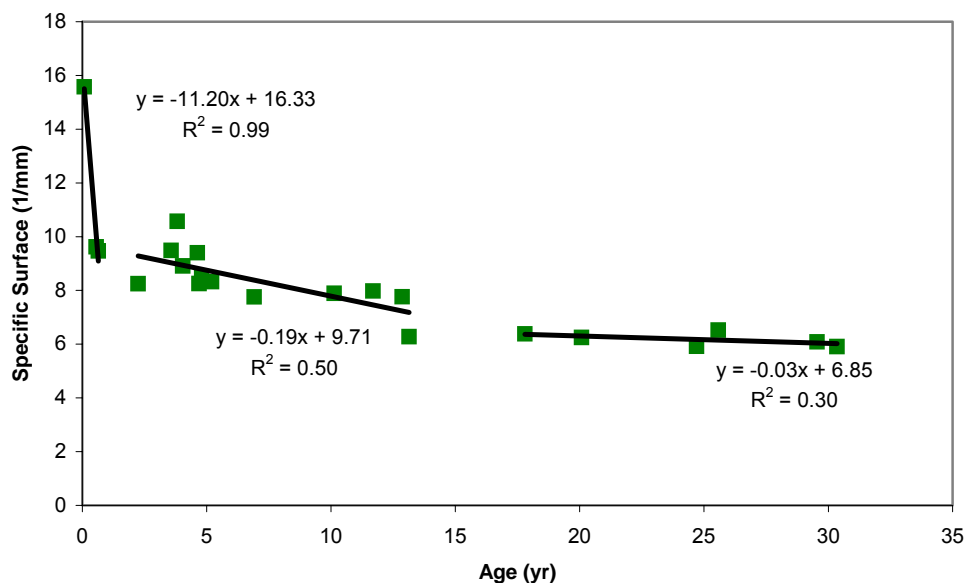


Figure 30. Specific surface decrease with time in the 2000-1 firn core.

the snowpack. Again, this part of the firn is subject to the strongest temperature gradients. Below the top meter, the reduction in specific surface becomes slow because the temperature in the firn is becoming smaller. Specific surface is an important parameter for chemical transport; large specific surface provides greater opportunities for surface sorption processes.

Figure 31 shows that the mean pore size increases at first and then very gradually decreases after a year in the 2000-1 core. Pore size increases near the surface because TG metamorphism creates large grains that push away from each other, destroying the necks between grains. Also, small grains are sublimating because of the large amount of vapor transport near the surface. Figure 31 shows that the pore size increases almost as rapidly as the grain size in the first year (Fig. 29).

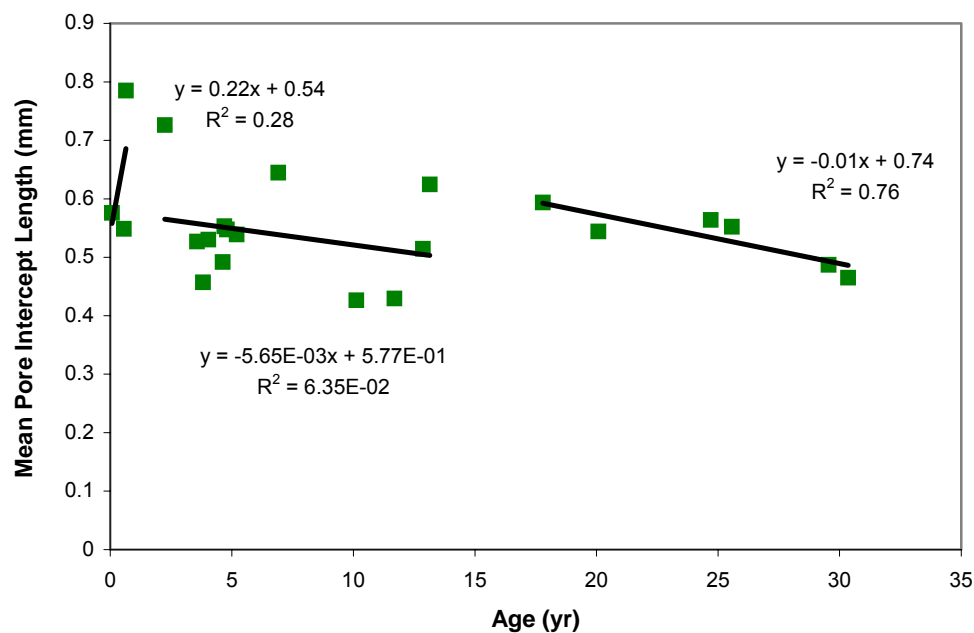


Figure 31. Pore size change with time.

The temporal changes in microstructure all follow a similar pattern. There is rapid change in the first year followed by more moderate and erratic change until a depth of 10 m is reached. Below 10 m the rates of change are much slower and linear with time because the firn temperature is nearly constant throughout the year.

Spatial Permeability and Microstructure Variations

Seven firn cores were extracted from seven geographic areas in West Antarctica. Elevation, topography, accumulation rate, and mean annual temperature vary between the sites (Table 1). It is important to know what variations in snow microstructure and permeability exist because of these varying influences. The permeability profiles of each of the seven firn cores vary widely from site to site (Fig. 32) and correspond with the amount and type of metamorphosis taking place within the snow. As mentioned before, the type and degree of metamorphism depend on the temperature and the strength of the temperature gradients. Gow (1968, 1969, 1971) and Gow et al. (1997) found that grain growth depends on temperature, accumulation rate, and local area strain rates caused by rapid ice movement. The last of these does not operate at shallow depths and does not cause metamorphosis in the firn cores analyzed here. Temperature and accumulation rate do, however, affect the snow metamorphism in all of these firn cores. Temperature and temperature gradients control the rate at which the snow grains grow and change shape due to vapor transport. Accumulation rate determines how long the snow grains are exposed to temperature gradients and air-snow transfer processes by the rate of burial.

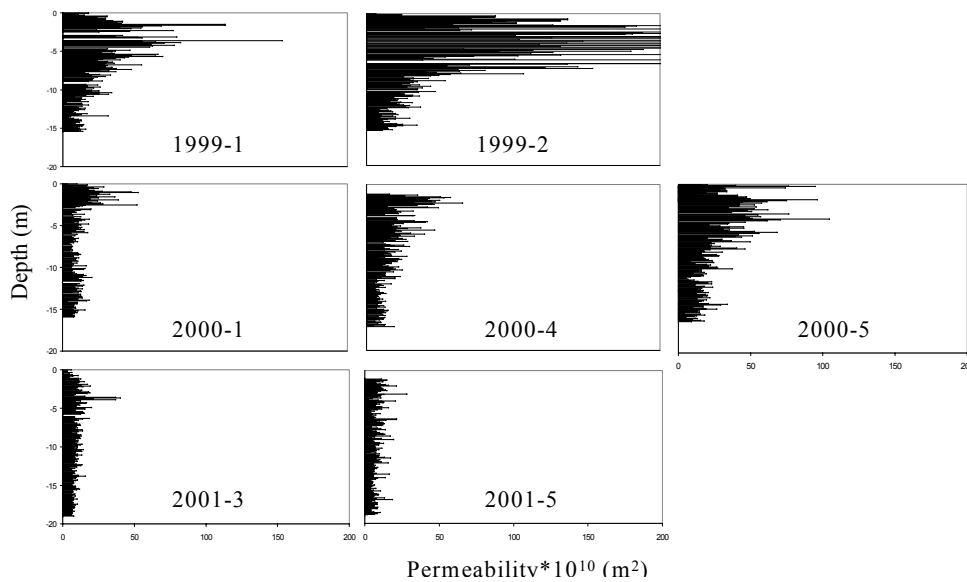


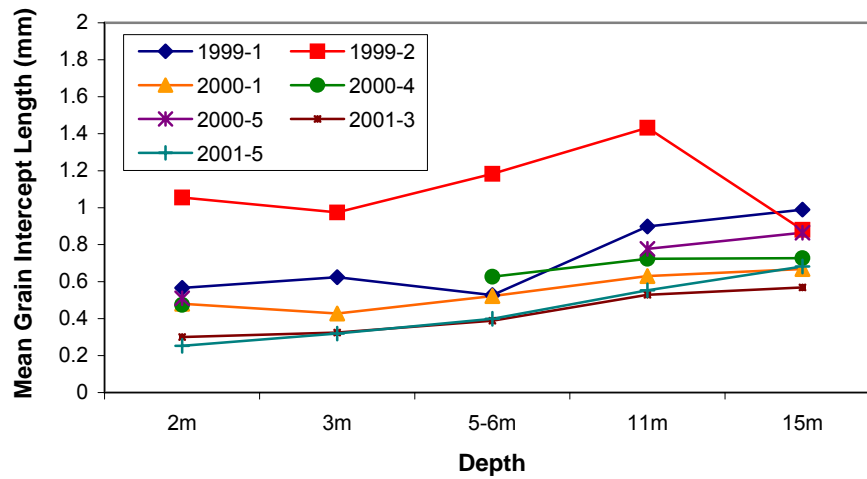
Figure 32. Permeability profiles of the ITASE firn cores. All permeability scales are the same to show site-to-site variations.

If an area has a high accumulation rate, then the snow gets buried faster and the snow grains spend less time in the near-surface region of rapid change due to

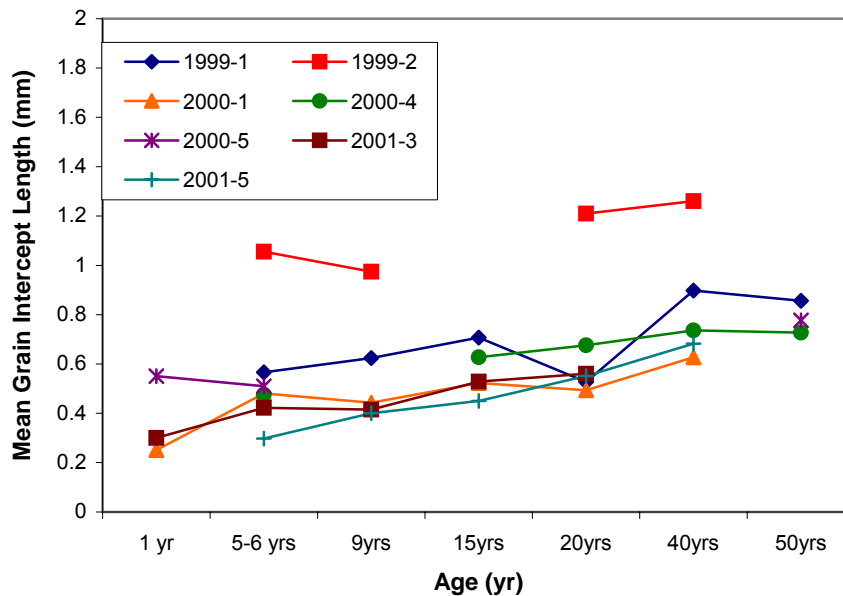
temperature gradients, leaving less time for TG metamorphism to take place. TG metamorphism opens up the pores and increases permeability. Thus, regions with high accumulation rates will have lower-permeability firn because less TG metamorphism has taken place. The cores extracted during 2001 confirm this. The accumulation rates of cores 3 and 5 of that year were 33.9 and 36.4 cm/year water equivalent, respectively (Table 1). This is two to three times greater than the accumulations rates for the 1999 and 2000 cores. The mean annual temperatures for sites 2001-3 and 2001-5 are between those of the 1999 and 2000 firn cores (Table 1), so a lower firn temperature is not the cause of the reduced metamorphism in these cores. Figure 28c shows that the overall permeability profiles of the 2001 cores are very low. The maximum around 2–3 m is nearly indistinguishable, especially in the case of core 5 (Fig. 32), and the pore and grain sizes are smaller than in the other firn cores (Fig. 33–36). Figure 36 shows how small the 2001 grains are compared to those of the 1999 and 2000 firn cores.

The reduced amplitude of the 2–3 m maxima in the 2001 cores is further evidence of less TG metamorphism (Fig. 32). The snow crystals do not change much from their original microstructure, so the permeability remains nearly constant relative to the behavior of the 1999 and 2000 cores. Figure 35a shows the near-surface wind pack of the 2001-3 core. Figure 35b shows a similar wind pack at 5 m. These images look very similar; the microstructure has not changed much with the first 5 m of depth. The cores from 1999 and 2000 show a very large change in microstructure over the first 5 m of depth. Figure 33 shows that the grains do not grow as large in the 2001 cores, and according to Figure 34, the pores are not opening up because of the lack of time spent in the TG metamorphism realm.

Accumulation rate is the primary control mechanism of microstructure and permeability. If mean annual temperature were the controlling mechanism, the 2001 firn cores should have permeability profiles and quantitative microscopy measurements between the 1999 and 2000 firn cores, which have higher and lower mean annual temperatures, respectively. If the accumulation rate between sites is similar, then mean annual temperature can be used to explain differences in microstructure and permeability.

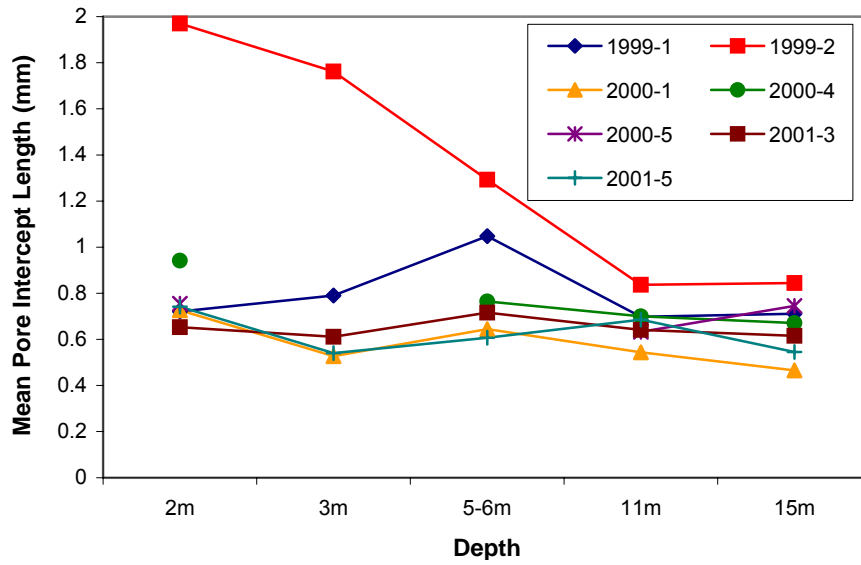


a. At similar ages.

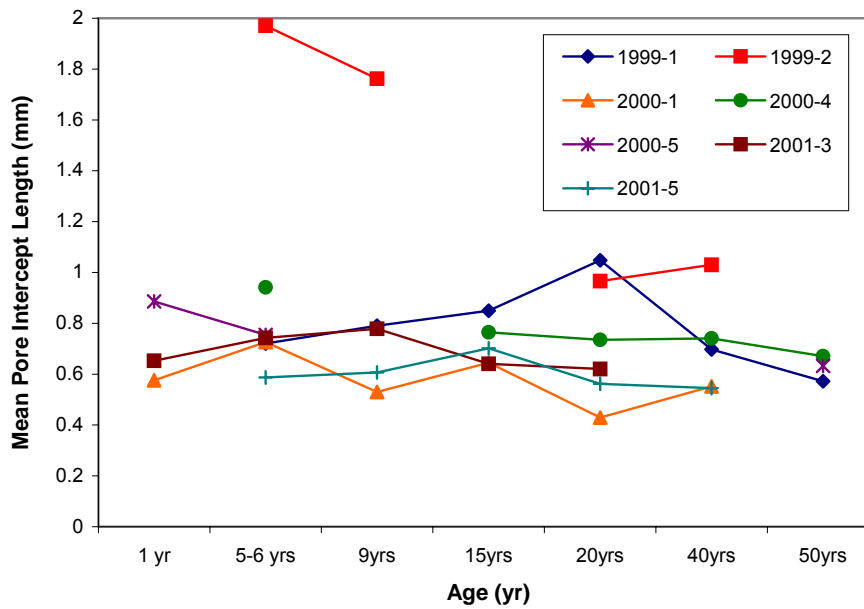


b. At similar depths.

Figure 33. Comparison of mean firn grain size increase for fine-grained firn at similar ages and depths. Missing data indicate that there was no homogeneous, fine sample at that age or depth. Note that the depth and age axes are not linear scales and are meant to compare the grain size of all firn cores at similar depths or ages.



a. At similar ages.



b. At similar depths.

Figure 34. Comparison of mean pore size at similar ages and depths. Missing data indicate that there was no homogeneous, fine sample at that age or depth. Note that the depth and age axes are not linear scales and are meant to compare the grain size of all firn cores at similar depths or ages.

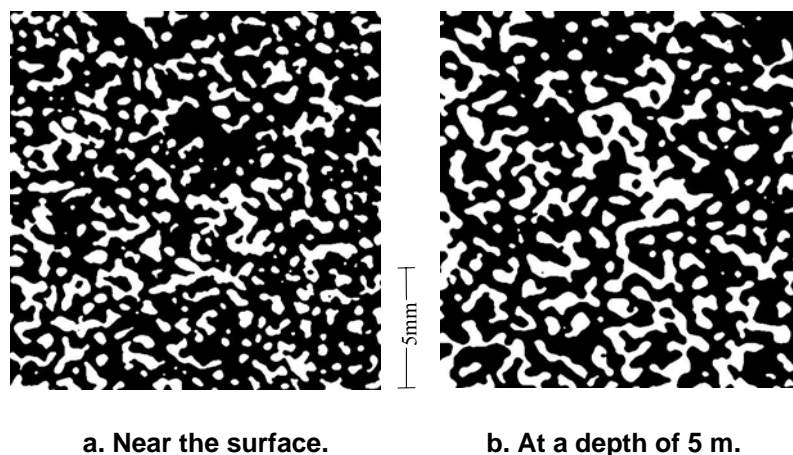


Figure 35. Comparison of 2001-3 firn near the surface and at 5 m. Stratigraphic up is to the left.

The cores extracted during 1999 and 2000 had much lower accumulation rates than the 2001 firn cores, between 11.9 and 17.3 cm/year (Table 1). The permeability profiles of these cores are all greater than those of the year 2001 (Fig. 32), suggesting more TG metamorphism and a greater amount of time spent above 10 m depths. The mean annual temperature of the sites accounts for the differences in permeability between the 1999 and 2000 firn cores (Table 1). The warmer the site, the faster that grain growth and metamorphosis can take place (Gow 1969, 1971). The firn core sites from the year 2000 all had mean annual temperatures around -29.5°C , which is lower than at the 1999-1 and 1999-2 sites, which had mean annual temperatures of -25.4°C and -21.5°C , respectively. Figure 31 shows that metamorphosis processes were slower at the 2000 firn core sites and as a result have smaller grains and pores (Fig. 33–36). Therefore, the permeabilities at these three sites were lower (Fig. 32). Of the cores from 1999, core 2 was warmer than core 1, so it had a much greater degree of metamorphosis. This is clear from the very high permeability of core 1999-2 and the very large grain and pore sizes visible in Figure 35. Core 1999-1 has a mean annual temperature of -25.4°C , which is between that of core 1999-2 and the 2000 cores. Thus, the 1999-1 permeability profile is less than 1999-2 but greater than all of the 2000 cores. The grain and pore sizes are also between the 1999-2 and 2000 cores (Fig. 33–36).

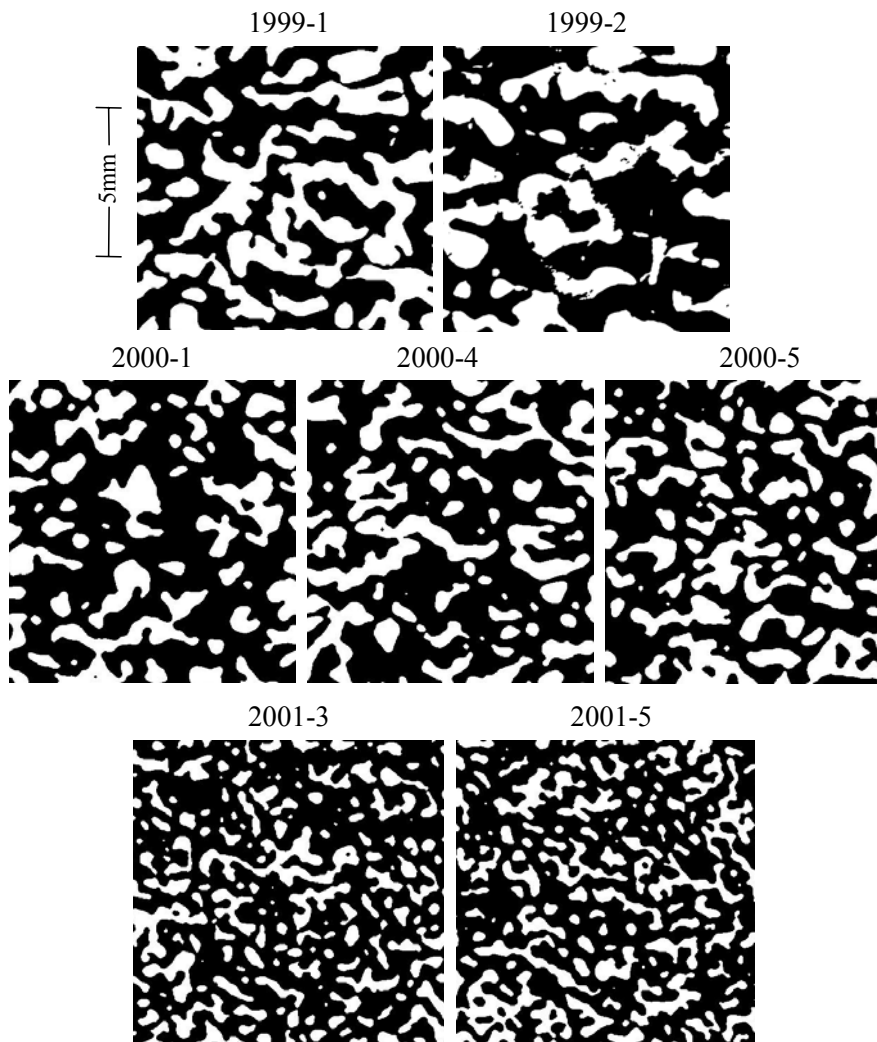


Figure 36. Digital images of all seven firn cores at a depth of 2 m. Stratigraphic up is to the left. This depth is in the region of maximum permeability.

Climate Indicators in Permeability and Microstructure

The original characteristics of the deposited snow grains will continue to affect them once they become buried. The surface grain sizes from the 2001 core are 50% smaller than those of the 2000 and 1999-1 cores, which may have contributed to the overall small microstructure and low permeability of the 2001 firn core. Naturally, at the same growth rate, grains that start out smaller will not become as large in the same amount of time. Many things can affect the size of

the surface grains. If a layer starts out as surface hoar, it will have large grains and large pores if the layer is buried undisturbed. However, that same surface hoar could be blown around in high winds, breaking the crystals and compacting them. A layer could also start out as snow from a storm and be buried as such, or it could become a sun crust before burial, resulting in a highly impermeable layer. Many of these effects are dampened out, but long-term changes in climate could result in a large section of the core having microstructural characteristics and permeabilities that differ from the rest of the core. If permeability is varying temporally, then the amount of ventilation into the firn is also varying over time.

The 2000 firn cores appear to exhibit such differences. These cores have more than one maximum in their permeability profiles. The deeper maxima in permeability are never of as great an amplitude as the shallow ones, but they reflect a change in the microstructure trends. The increase in permeability in deeper layers is most apparent in the 2000-1 core.

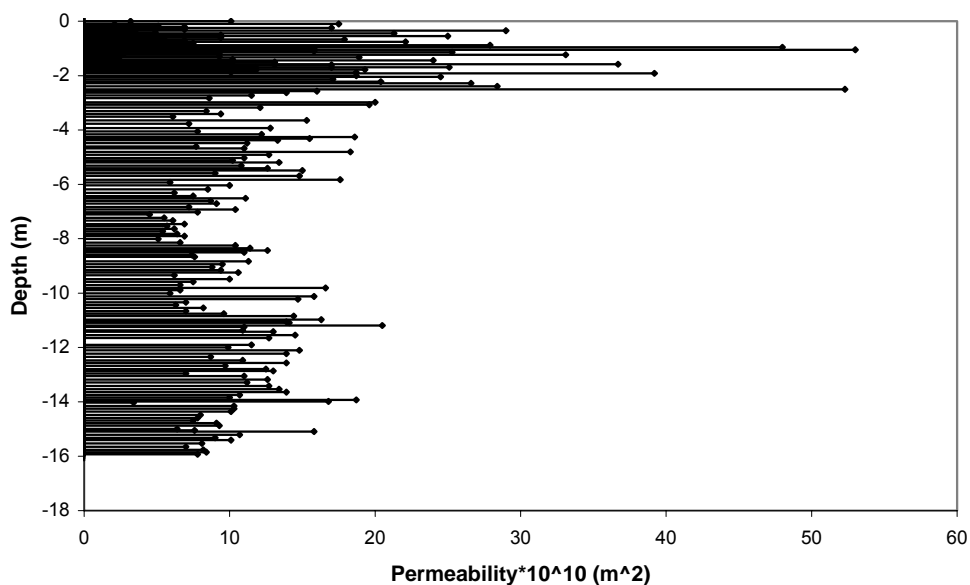


Figure 37. 2000 firn core permeability profiles illustrating multiple maxima.

Figure 37 shows the second maximum in the 2000-1 core beginning around 8.5 m and reaching its highest values around 12 m. Several quantitative microscopy irregularities were found to occur at 8 m in this core in addition to the increase in permeability. The mean grain intercept length increases suddenly in almost a step fashion at 8.5 m (Fig. 38). This is easier to see when looking at one type of microstructure, so Figure 38 contains fine-grained samples only.

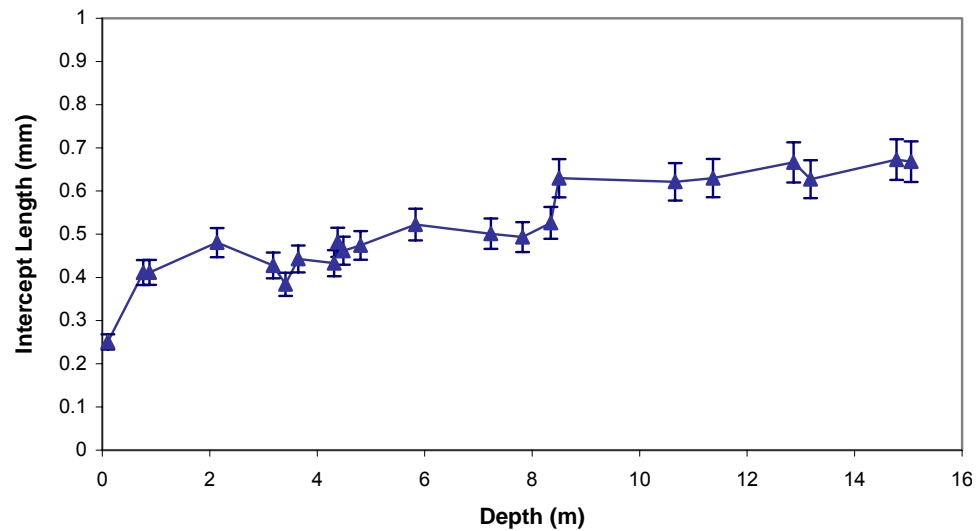


Figure 38. Mean grain intercept length increase with depth of the 2000-1 firn core. Note the abrupt increase in grain size at 8.5 m.

The pore size trend also abruptly changes at 8.5 m. Around 8.5 m in the absence of a change in accumulation rate, temperature, or shear stress, the pore size should be gradually decreasing because of the overburden pressure, as it does in the other firn cores (Fig. 12). However, in the 2000-1 core the trend of decreasing pore size with depth is interrupted by an abrupt pore size increase at 8.5 m (Fig. 39).

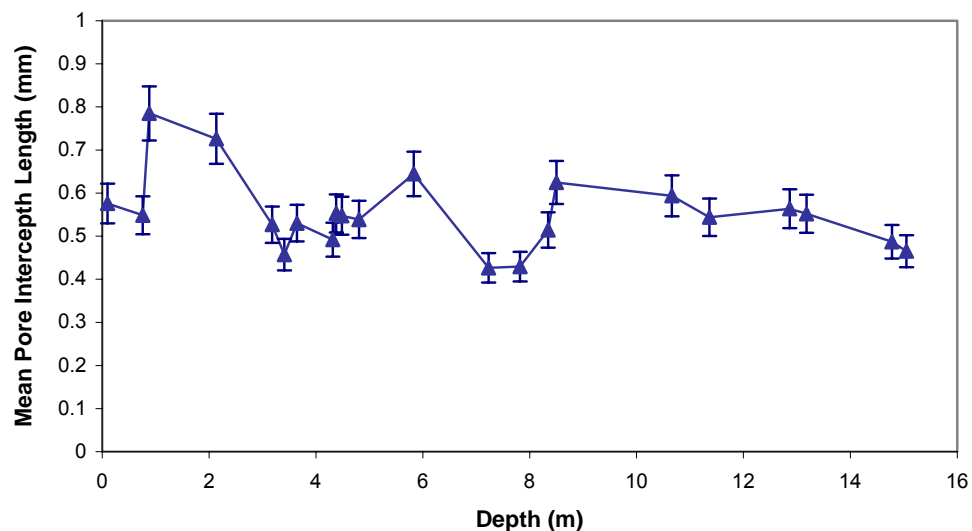


Figure 39. Mean pore intercept length with depth for the 2000-1 firn core. Note the abrupt increase at 8.5 m.

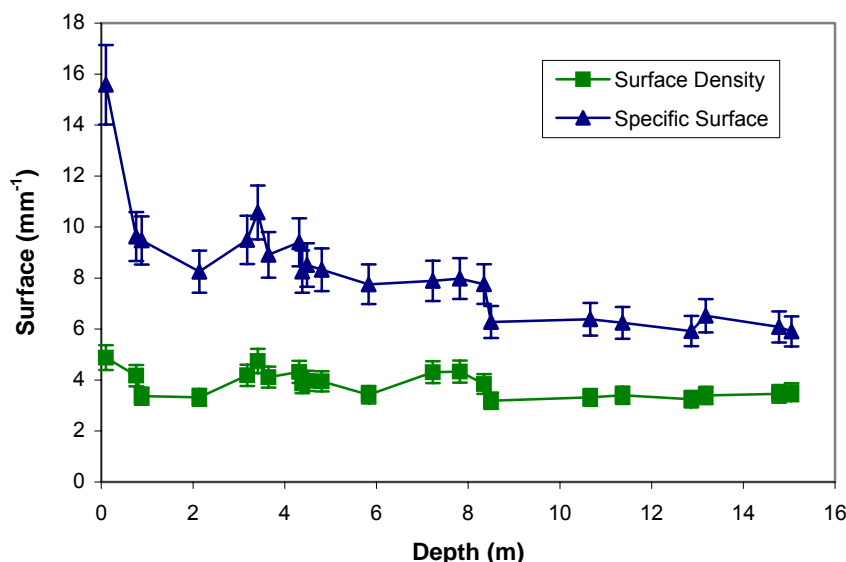


Figure 40. Surface characteristics with depth for the 2000-1 firn core. Note the sudden decrease in surface at 8.5 m.

Along with grain and pore size, the specific surface and surface density exhibit a sudden change at 8.5 m. It can be seen in Figure 40 that both measurements of surface decrease suddenly at 8.5 m. Figure 41 shows images of fine-grained firn above and below 8.5 m. We would expect the deeper image to have similar mean grain and pore sizes since the samples are very close to each other in the firn, but the sample below 8.5 m clearly exhibits much larger grains and pores than the shallower sample.

There could be several reasons for the different firn microstructure below 8 m in the 2000-1 firn core. The age of the firn at 8 m in this core is 13 years. At the second maximum in the permeability profile, the age of the firn is 20 years. The site may have been warmer prior to 20 years ago, causing faster near-surface grain growth. Once buried, the grains would continue to grow. However, if the site experienced lower mean annual temperatures in more recent years, the snow at the surface would grow slower in the cooler conditions.

Another meteorological impact of climate change could have been the rate of accumulation of the snow. If snowfall was less frequent 20 years ago, that surface snow would be in the realm of TG metamorphism for a longer time, and the amount of rapid grain growth would have increased. As snowfall became more frequent since then, surface snow would be buried faster and would not experience as much TG growth, resulting in smaller microstructure.

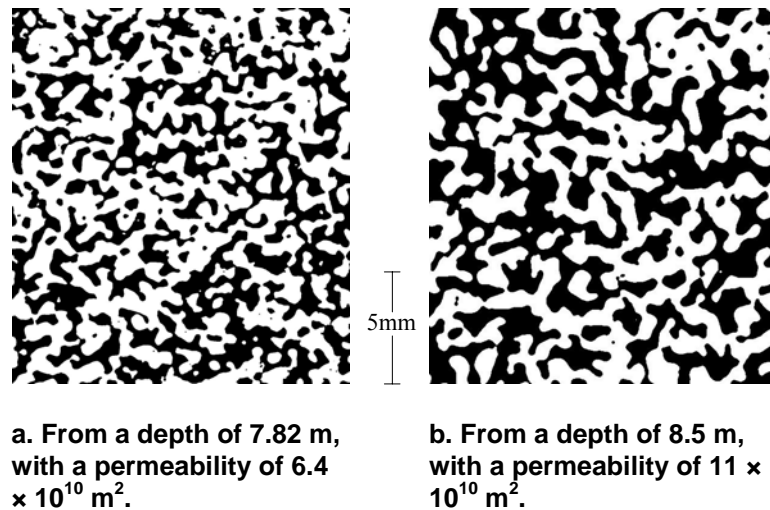


Figure 41. Images showing the abrupt increase in mean grain and mean pore sizes and the decrease in surface area.

One more cause of gross microstructural changes in a firn core could be movement of an ice divide. Ice divides are similar to continental divides in that weather systems are affected by them and they influence the direction of flow of any fluids originating in their area. Ice divides are different because they can move and the flowing material is the ice itself. The ITASE sites of 2000 surrounded an ice divide, which has probably moved in the last several hundred years. Several important weather circulation patterns cross this divide, and the prevailing winds run perpendicular to it. If a region of firn was located on the windward side of this divide 100 years ago, high wind would cause increased metamorphism and scouring of the surface, which results in rapid grain growth. As the divide moves and the surface snow becomes buried, this same region may move to the leeward side of the divide. The newer snow at the surface would be buried faster and less metamorphosis would have take place, resulting in smaller microstructure. The deeper snow would have large microstructure because of its previous location on the other side of the divide. This might lead to an increase in permeability deeper in the core instead of the usual decrease with depth.

However, the transition to different microstructure seen at 8.5 m in the 2000-1 firn core is most likely not attributable to the movement of an ice divide. Ice flow is extremely slow, and the time required for an ice divide to change position is at least 75–100 years if not longer.* The sudden changes in microstructure and the second permeability maximum are most likely caused by climate changes. Accumulation rate data for the 2000-1 ice core shared by Debra Meese indicate

* Personal communication with Dr. Steven Arcone, CRREL, 2002.

a decrease in accumulation around 20 years ago, which corresponds to the beginning of the second increase in permeability and the anomalous changes in microstructure. This leads to the conclusion that the amount of ventilation in the firn at the 2000-1 site has varied through time and began to decrease about 20 years ago.

Variations in ventilation with time have a potential impact on rapid climate change studies using ice cores. Increased ventilation serves to smooth the ice core record of many chemical species and isotopes by mixing in the upper layers of the firn. An example of this is the isotope record found in the ice and snow layers of an ice core. Snow grains are deposited onto the surface with an $\delta^{18}\text{O}$ concentration representative of that found in the water vapor of the atmosphere directly above the site of deposition. That concentration does not remain constant, however, due to ventilation. As air flows past the individual snow grains, the isotopes can diffuse through the grain and then sublimate into the moving air (Waddington et al. 2002). Lighter isotopes will preferentially sublimate over heavier ones, so the remaining snow grain will become enriched in $\delta^{18}\text{O}$. Thus, sites with more ventilation (lower accumulation) have $\delta^{18}\text{O}$ concentrations greater than those found in the atmosphere at the time of deposition. The same phenomenon will occur for δD isotope concentrations in the snow.

Gas bubble concentrations are also affected by changing ventilation. Sowers et al. (1992) found that the Vostok core, a site with very low accumulation, had relatively high $\delta^{15}\text{N}$ enrichment compared to ice cores from sites with higher accumulations. Below the convection zone, the air diffuses down into the firn, and the heavier nitrogen isotopes, ^{15}N , preferentially travel deeper because of gravity. It may be possible that the rate of diffusion will be affected by the firn microstructure. A site with very low accumulation, such as Vostok, has microstructure that has undergone significantly more metamorphism than any of the ITASE sites, which have higher accumulation rates. Perhaps the ^{15}N signature at Vostok has been affected by the coarsening of the firn and subsequent effects on diffusion rates.

These examples are just two of the effects that changing microstructure might have on the interpretation of ice cores. Quantification of microstructure characteristics and ventilation may greatly aid in a more accurate interpretation of chemical records in ice cores. Efforts at modeling diffusion, airflow, and chemistry transport through different types of firn are currently taking place, and the permeability and microstructure data presented in this report will be used in such models.

Predicting Permeability from Microstructure

Modeling of air–snow transport processes requires the use of several snow parameters, including permeability. The accuracy of the models depends on how closely the parameters used in it represent reality in the firn. It would be extremely beneficial to be able to predict permeability from microstructure for use in these models. At remote sites it is far easier to collect microstructure samples than to do permeability measurements. Previous studies done to correlate permeability of snow or soils with microstructure have focused on parameters such as grain size, density, or porosity (Shimizu 1970, Revil and Cathles 1999). The results have been inadequate at predicting the transport properties of polar snow from microstructural characteristics (Luciano and Albert 2002). Shimizu (1970) proposed the following formula for permeability of fine-grained, compact snow:

$$B_o = 0.077d_o^2 \exp(-7.8\rho_s^*) \quad (18)$$

where B_o = permeability
 d_o = mean grain size (cm)
 ρ_s^* = specific gravity of the snow.

This formula underestimates the permeability of the snow in the ITASE firn cores and does not work well for snow of coarse microstructure. Figure 42 shows the comparison between the measured permeability and that predicted by Equation 18 using quantitative microscopy statistics. The Shimizu (1970) formula also does not predict the large increase in permeability near the surface.

Revil and Cathles (1999) investigated the permeability of soils by using the analogy of electrical conduction theory to improve upon the Kozeny–Carman (KC) relationship for permeability (Eq. 19). The KC relationship states that the permeability is related to the grain radius and the porosity. The Revil and Cathles (1999) analysis recognizes that not all pores are open to airflow and that there is an “effective porosity” that is a fraction of the total porosity. There must also be an “effective hydraulic radius” to address the issue of throat size. Smaller throat size will decrease the amount of flow possible. The final equation Revil and Cathles produced by analyzing soil data from sands was Equation 20.

$$k = \frac{\phi}{2} \left(\frac{R}{2} \right)^2 \quad (19)$$

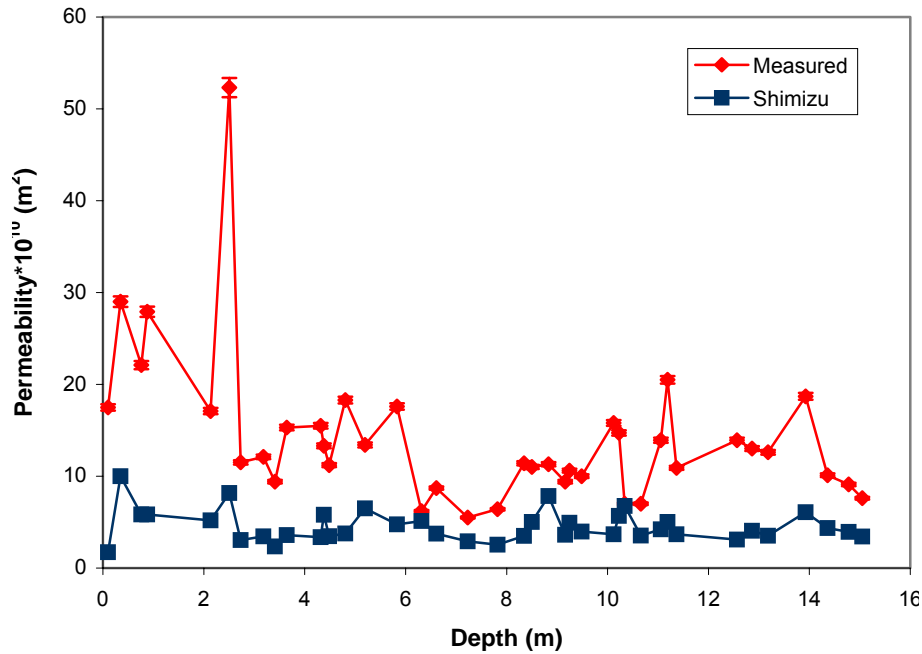


Figure 42. Permeability predicted by the Shimizu (1970) formula using microstructural characteristics and measured permeability.

$$k_{\text{sand}} = \frac{R^2}{2m_{\text{sand}}^2 F^3} \quad (20)$$

where k = permeability
 R = grain radius
 m = cementation exponent with a value between 1 and 4
 F = electrical formation factor.

The formation factor is related to the cementation exponent by the Archie relationship:

$$F = \phi^{-m} \quad (21)$$

where ϕ is the porosity. According to Revil and Cathless (1999), the KC equation overestimates the permeability of sand. By adjusting m in Equation 20, they can better predict the permeability of sand. Increasing m decreases the permeability predicted by the KC equation.

For snow the KC equation also overestimates the permeability. Figure 43 shows the permeability of the ITASE samples predicted by the KC relationship. The KC relationship does a slightly better job than Shimizu (1970) for predicting the large increase in permeability near the surface. The Revil and Cathless relationship (Eq. 20) was applied to the ITASE 2000-1 firn samples using the lowest value of the range of m , $m = 1$. Figure 44 shows that this equation predicts snow permeabilities fairly well below 5 m in the core, but as in the first two relationships, the high permeability near the surface is not predicted. Also, using a value of $m = 1$ in Equation 20 appears to overcompensate for the KC relationship, so it would be better to use values of $m < 1$, which is out of the suggested range in Revil and Cathless (1999). Equation 20 was determined for sand, and the metamorphism of the snow is a feature of porous media that makes it different from sand. The development of such an equation for snow may require further adjustments to the Revil and Cathless equation.

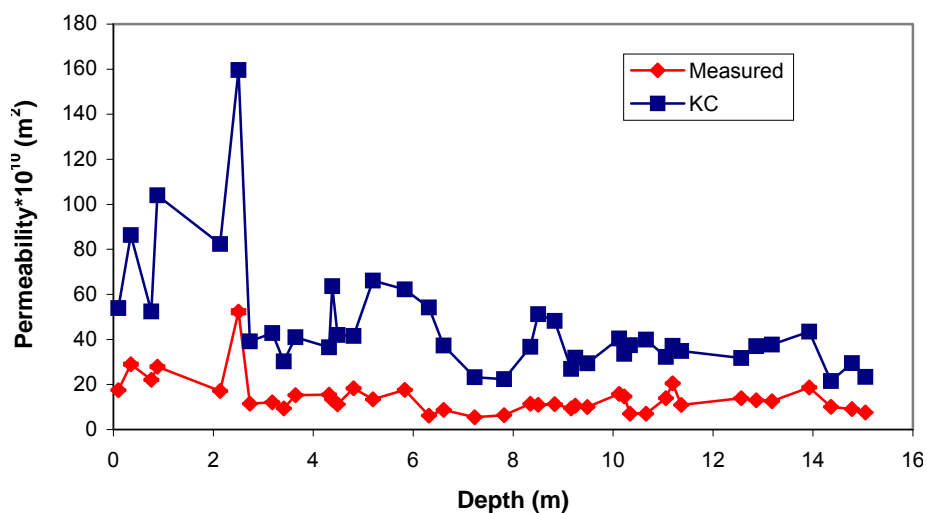


Figure 43. Permeability predicted by the KC equation versus measured permeability.

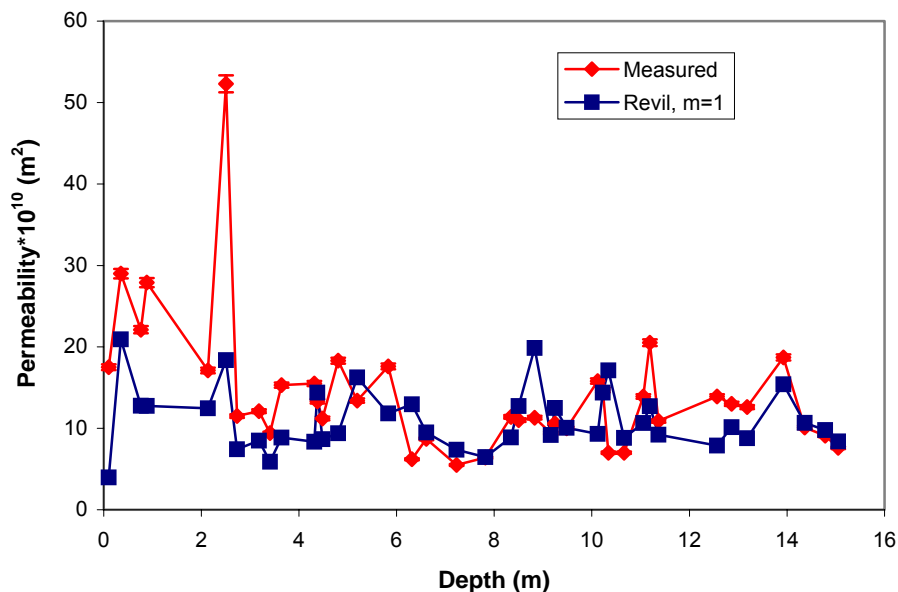


Figure 44. Permeability predicted by Revil and Cathless (1999), with the cementation factor $m = 1$, versus measured permeability.

Density and grain size increase with depth, while porosity decreases with depth. From the equations above it can be seen that these are properties commonly used to predict permeability. However, none of these parameters exhibit the same profile as permeability does with depth, so they cannot be the only things controlling transport through the snow. Figure 45 shows the increase in grain size and decrease in pore size with depth, along with the permeability changes with depth. Air travels through the pore spaces in snow, so one must concentrate on the pores to gain a better understanding of what controls airflow. Naturally, grain size and porosity will have an effect on permeability, especially at great depths, where the overburden pressure compresses the snow grains. Growing grains in this environment constricts the network of pores, reducing porosity and permeability. However, grain size and porosity tell a small piece of the story. Pore size and shape play an important role in determining the permeability of snow.

By comparing the permeability profiles with those of microstructural measurements of core 2000-1, we can investigate the relationship between them. One of the most important characteristics of the pores is their specific surface, or surface-to-volume ratio. In the 2000-1 core the permeability will decrease if the specific surface increases or if the volume-to-surface ratio decreases (Fig. 46). The pore volume-to-surface ratio follows the same trend as permeability, with an increase until about 2.5 m and then a decrease to greater depths. The volume-to-

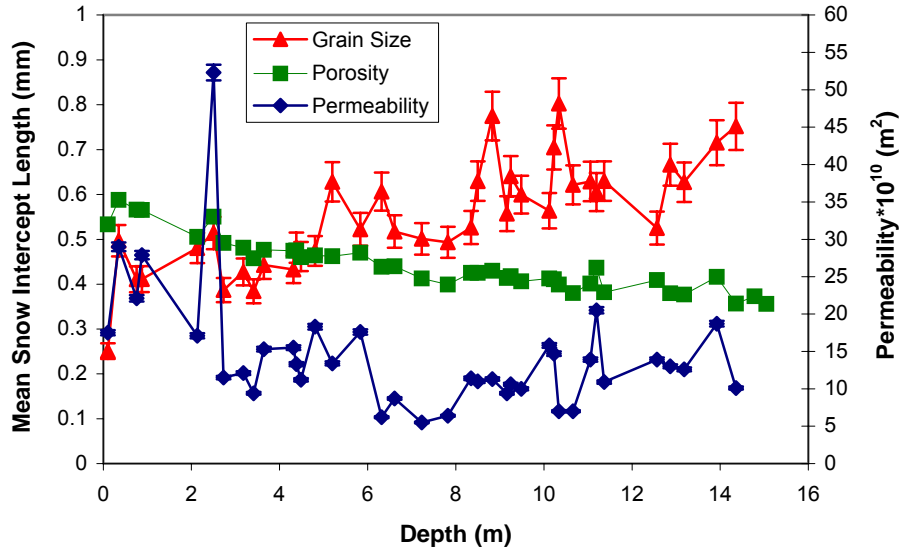


Figure 45. Grain size and porosity increase with depth, which does not follow the permeability pattern of increase and then decrease.

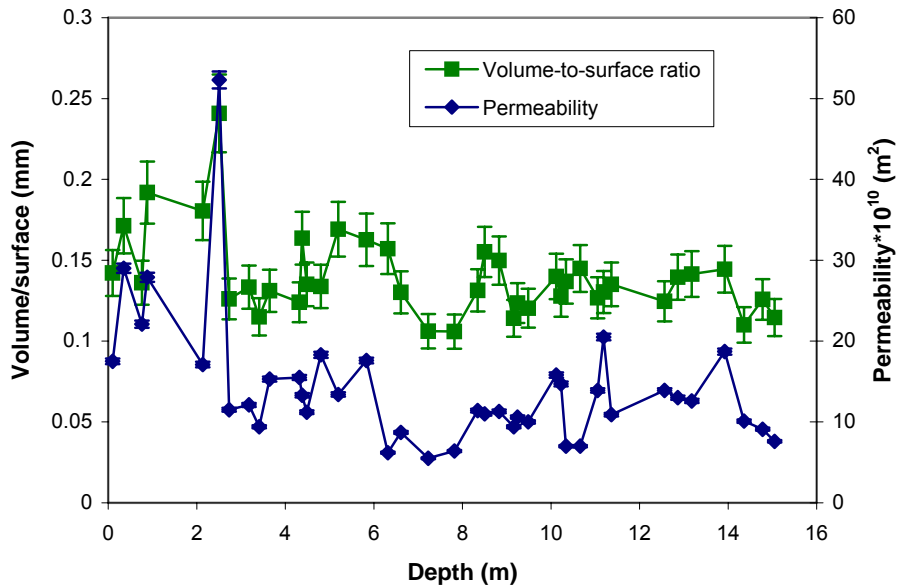


Figure 46. Volume-to-surface ratio of the pores in the 2000-1 firn core. Note the similarity between the permeability and volume-to-surface curves.

surface ratio of the grains generally increases, which is to be expected as ET metamorphism takes place. Soon after deposition, the volume-to-surface ratio of the pores increases because the amount of pore surface is decreasing as small grains disappear and the remaining grains become more rounded. The consuming of small grains by large grains also increases the volume of the pores.

Because the pore characteristics correlate well with permeability, it would appear that pore measurements should be used in formulas attempting to predict permeability. Several attempts were made to develop a relationship between permeability and microstructure that improves upon other formulas. Using our data, we developed the following formula, which predicts snow permeability better than Shimizu (1970) and Revil and Cathless (1999):

$$k = d_{\text{pore}} \left(\frac{\phi}{4} \right)^2 \left(\frac{V}{S} \right)_{\text{pores}} \quad (22)$$

where d = mean pore intercept length
 ϕ = porosity
 V = volume fraction
 S = surface density.

In the field, permeability measurements of the same layer of snow vary by about 10%, so predicting permeability using microstructure characteristics would ideally fall within 10% of the measured value. Figure 47 shows that Equation 22 predicts the large increase in permeability around 3 m but significantly underestimates the permeability in most samples below 9 m in the 2000-1 core. The percent error is plotted in Figure 48, and the general increase in error with depth is evident.

Figure 47 compares the permeability predicted by Equation 22 to the measured permeability of both fine and coarse snow samples. This is beneficial because all previous formulas developed for permeability only work for very specific types of snow. This equation also works reasonably well for the other firn cores. Figures 49–51 show the measured permeability versus the permeability predicted by Equation 22 for all of the ITASE cores. It does not predict the permeability near the surface of the 1999 cores very well, and it overestimates the permeability of core 2001-5. However, it does predict the permeability of the 2000 cores fairly well, and it does predict the maximum permeabilities found in the top few meters of each core.

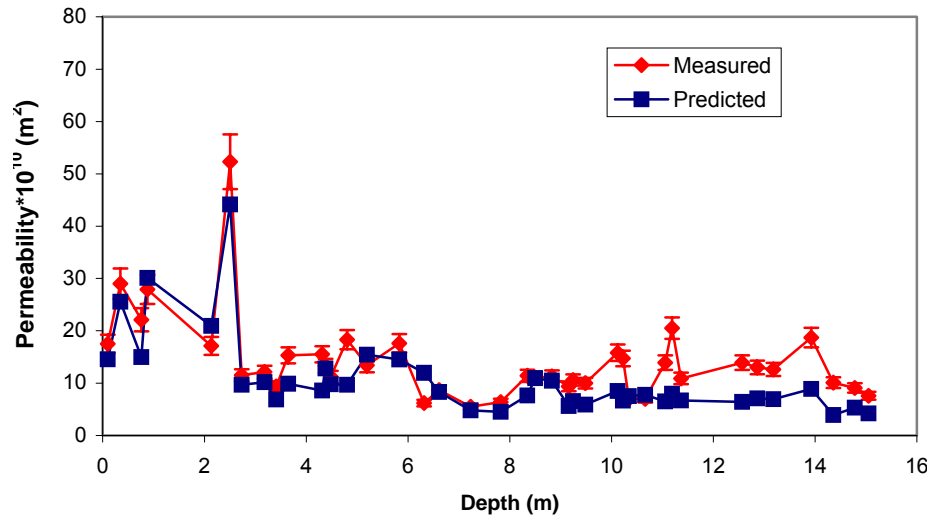


Figure 47. Permeability predicted by Equation 22. The error bars are 10% because the natural variation in permeability of a specific layer has been found to be 10%.

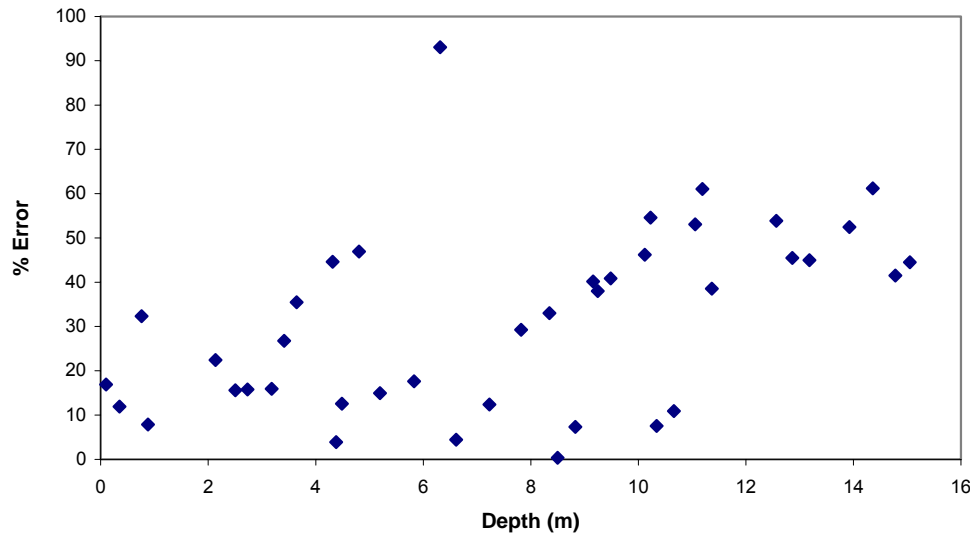


Figure 48. Percent error of each sample permeability predicted by Equation 22.

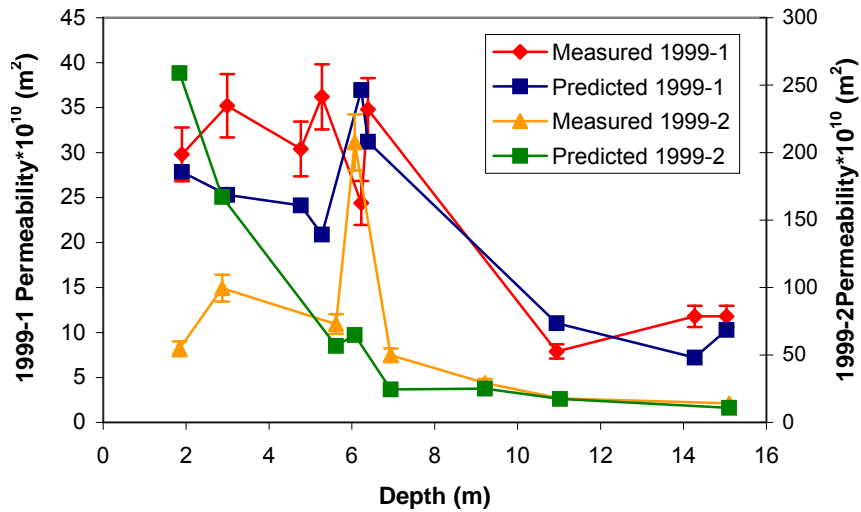


Figure 49. Permeability of 1999 firn cores predicted by Equation 22. The error bars on measured values are 10%. Each core is measured on its own axis because of the very high permeability of core 1999-2.

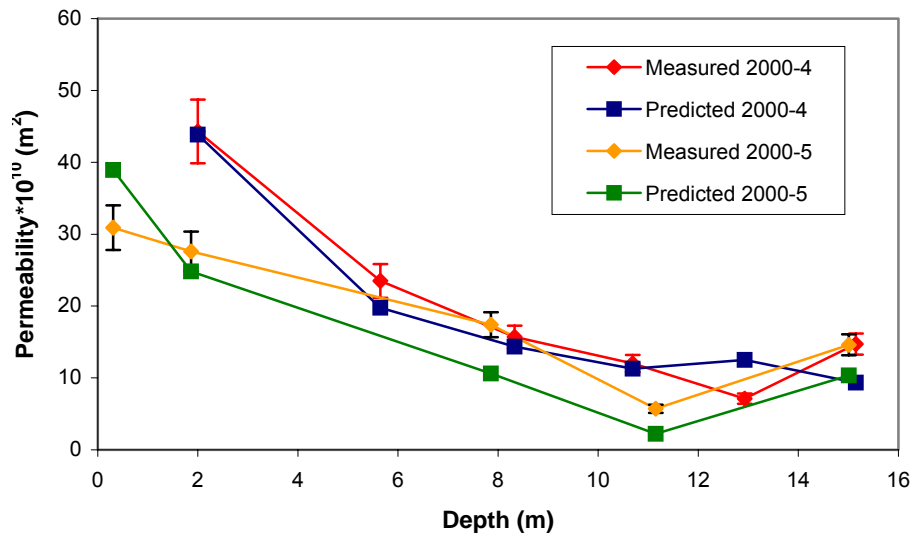


Figure 50. Permeability of 2000 firn cores predicted by Equation 22. The error bars on measured values are 10%.

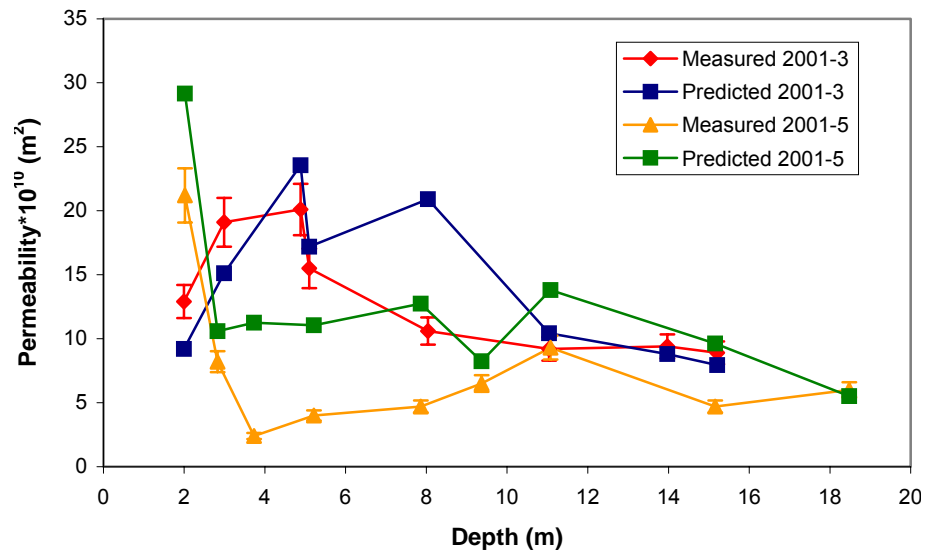


Figure 51. Permeability of 2001 firn cores predicted by Equation 22. The error bars on measured values are 10%.

Equation 22 does a reasonable job of predicting permeability of polar firn, and it gives the gross shape of the measured permeability profiles. Clearly, more work needs to be done on a formula to predict permeability from the microstructure. Perhaps depth or age will have to be included, or some combination of Equation 22 and the Revil and Cathles equation is needed. The ratio of pore size to grain size may also be important. Many forces cause changes in the microstructure and therefore the permeability, but it would be most convenient to limit the variables in the equation to those that can be easily measured from firn samples.

6 CONCLUSION

Seven firn cores drilled in West Antarctica provide the opportunity to investigate the natural variability of snow and firn microstructure and the impact it has on firn permeability. Permeability and quantitative microscopy measurements were made on the cores, and the permeability was related to the microstructure. Microstructural changes with time and spatial differences were used to explain similar variations in permeability with depth and from site to site.

Both the permeability and microstructure vary greatly from site to site, indicating that differences in firn microstructure and air–snow transport processes are likely to affect ice core interpretation. The firn at the 2001 sites had very low permeability and relatively small mean grain and mean pore sizes. The low permeability can be explained by the small amount of temperature gradient (TG) metamorphism that has affected the microstructure in the 2001 cores, leaving the pores small and the necks between snow grains intact. The surface snow is exposed to seasonal and diurnal temperature gradients, causing grain and pore growth near the surface. These temperature gradients only remain strong enough to drive TG metamorphism down to a depth of about 20 cm.

The small degree of TG metamorphism affecting the 2001 firn cores can be largely attributed to very high accumulation rates at these sites. The snow is buried quickly and does not spend much time where temperature gradients are strong enough to drive TG metamorphism and where surface processes such as ventilation exist. The case of the 2001 cores shows that accumulation rate is the mechanism controlling microstructure. The moderate temperatures of the 2001 firn core sites were not enough to cause much grain growth and metamorphism. The remaining firn cores had much lower accumulation rates, but their permeability profiles and microstructures were still different from each other. The mean annual temperatures of the sites cause the grains to grow at differing rates, thereby affecting the permeability. Metamorphism occurs more rapidly with higher temperatures because warmer air can hold more water vapor than colder air. The 1999-2 core has the highest mean annual temperature of all of the cores, causing the grains to grow rapidly and the pores to open up by the small grain sublimation. Consequently this core has the highest permeability by far. The 2000 firn cores have the lowest mean annual temperatures and therefore less TG metamorphism. They also have lower permeabilities than the 1999 firn cores.

In addition to the magnitude, the shape of the permeability profile can be explained by microstructure and metamorphism. In all of the cores, the permeability increases with depth down to about 3 m. Then it gradually decreases with depth. This decrease in permeability cannot be attributed to compression failure

due to the overburden pressure. Near the surface, TG metamorphism causes grain and pore growth and the destruction of the necks between grains. This increases the ease of airflow through the firn and thus permeability.

Below the top several centimeters in the core, the temperature differences between firn layers are not strong enough to drive TG metamorphism, and equitemperature (ET) metamorphism takes over. ET metamorphism causes rounding and sintering of the snow grains. This low-temperature gradient grain growth is slower than TG growth and is linear with time below 10 m, where the temperature of the firn changes little throughout the year. Above 10 m the grain growth is still slow, but it is faster than below 10 m because it experiences seasonal temperature fluctuations. ET metamorphism is faster when the temperature is higher. The grains continue to grow and sinter together with depth. This metamorphism causes steadily decreasing permeability with depth in the firn cores.

The 2000-1 firn core presents some exceptions to the usual steady decrease in permeability below 3 m. The permeability increases to another maximum at 12 m, or 35 years, in the 2000-1 core. The second maximum is of much smaller amplitude than the first, but it is still significant. The microstructure of the 2000-1 core shows large changes at 8 m, which is where the permeability begins increasing with depth in the 2000-1 core. The grain and pore sizes exhibit a marked increase, while the surface decreases very suddenly at 8 m. These differences in microstructure are likely due to the original conditions present when this snow was deposited. In the past the accumulation rate may have been lower, causing the surface snow to experience more metamorphism. Or the mean annual temperatures could have been higher, resulting in faster grain growth. The second maximum in permeability of the 2000-1 core is likely due to accumulations rates that were lower 20 years ago than in more recent times. Once the isotope and chemistry data are complete for the 2000-1 ice core, we will be able to determine whether there is a climate change associated with the microstructure changes at 8 m in this core.

Traditionally grain size and density have been used in attempts to predict snow permeability. However, these were only successful for fine-grained, seasonal snow. We investigated relationships between microstructure and permeability. Grain size and density increase with depth and do not follow the same trend as permeability. The pore size and pore specific surface do follow the increase and subsequent decrease in permeability. An equation was developed that can be used to predict the permeability of the firn using porosity, pore size, and pore specific surface for polar firn above 20 m. It is not known how well this formula will predict the permeability of deeper firn since the firn cores were not longer than 20 m. This formula was reasonably good at predicting the gross shape of the permeability profiles and was best at predicting the permeability of

the 2000 cores. The formula appears to slightly overestimate the permeability of the shallow firn and underestimate the permeability of the deeper firn. More work is needed to develop a truly usable formula. However, a good start was made here.

More research will be useful for increasing our understanding of relationships between microstructure and permeability. Additional investigations into quantitative microscopy will fill in the gaps and perhaps aid in finding a formula to predict permeability from microstructure. It would be useful to know whether the equation developed here will hold true once the entire microstructure of a core is known. In this study, only samples of homogeneous microstructure were used. Firn samples with layers can also be investigated to find the dependence of permeability on layering. The effect layering has on the permeability of a sample of several layers is important for a complete understanding of how air flows through the firn.

The U.S. ITASE is a continuing project, and in the 2002 field season firn cores were drilled on a route from Byrd Station to the South Pole, which is on the Antarctic plateau. At the time of this report, the cores had not yet arrived for analysis. The firn at these very high and very dry elevations will be very different from the firn in West Antarctica. Future field seasons of the U.S. ITASE will increase our understanding of microstructure, its effect on permeability and air-snow transport processes, and ice core interpretation for investigations of linked physical-chemical exchange.

REFERENCES

Abele, G. (1990) Snow roads and runways. CRREL Report M90-03, U.S. Army Cold Regions Research and Engineering Laboratory, Hanover, N.H.

Abele, G., and A. Gow (1975) Compressibility characteristics of undisturbed snow. Research Report 336, U.S. Army Cold Regions Research and Engineering Laboratory, Hanover, N.H.

Albert, M.R. (1993) Numerical experiments on firn ventilation with heat transfer. *Annals of Glaciology*, **18**: 161–165.

Albert, M.R. (1996) Modeling heat, mass and species transport in polar firn. *Annals of Glaciology*, **23**: 138–143

Albert, M.R. (2002) Effects of ventilation on sublimation rates in snow and firn. *Annals of Glaciology*, **35**: 52–56.

Albert, M.R., and R. Hawley (2000) Seasonal differences in surface energy exchange and accumulation at Summit, Greenland. *Annals of Glaciology*, **31**: 387–390.

Albert, M.R., and R. Hawley (2002) Seasonal changes in snow surface roughness characteristics at Summit, Greenland: Implications for air–snow transfer processes. *Annals of Glaciology*, **35**: 510–514.

Albert, M.R., and E.F. Schultz (2002) Snow and firn properties and air–snow transport processes at Summit, Greenland. *Atmospheric Environment*, **36**: 2789–2797.

Albert, M.R., E.M. Arons, and R.E. Davis (1996) Firn properties affecting gas exchange at Summit, Greenland: Near-surface ventilation possibilities. In *Chemical Exchange Between the Atmosphere and Polar Snow* (E.W. Wolff and R.C. Bales, ed.), NATO ASI Series I, **43**: 561–571.

Albert, M.R., E.F. Shultz, and F.E. Perron (2000) Snow and firn permeability at Siple Dome. *Annals of Glaciology*, **31**: 353–356.

Albert, M.R., A.M. Grannas, J. Bottenheim, P.B. Shepson, and F.E. Perron (2002) Processes and properties of snow–air transfer in the high Arctic with application to interstitial ozone at Alert, Canada. *Atmospheric Environment*, **36**(15–16): 2779–2787.

Alley, R.B. (1988) Concerning the deposition and diagenesis of strata in polar firn. *Journal of Glaciology*, **34**(118): 283–290.

Alley, R.B., and C.R. Bentley (1988) Ice core analysis on the Siple Coast of West Antarctica. *Annals of Glaciology*, **11**: 1–7.

- Alley, R.B., J.F. Bolzan, and I.M. Whillans** (1982) Polar firn densification and grain growth. *Annals of Glaciology*, **3**: 7–11.
- Alley, R.B., E.S. Saltzman, K.M. Cuffey, and J.J. Fitzpatrick** (1990) Summertime formation of depth hoar in central Greenland. *Geophysical Research Letters*, **17**(12): 2393–2396.
- Arons, E.M.** (1994) Dependence of snow thermal and electrical conductivities on microstructure. PhD thesis, Dartmouth College, Hanover, N.H.
- Bottenheim, J.W., J.E. Dibb, R.E. Honrath, and P.B. Shepson** (2002) Editorial, An introduction to the Alert 2000 and Summit 2000 arctic research studies. *Atmospheric Environment*, **36**(15–16): 2467–2469.
- Cabanes, A., L. Legagneux, and F. Domine** (2002) Evolution of the specific surface area and of crystal morphology of Arctic fresh snow during the ALERT 2000 campaign. *Atmospheric Environment*, **36**(15–16): 2767–2777.
- Clarke, G.K.C., and E.D. Waddington** (1991) A three-dimensional theory of wind pumping. *Journal of Glaciology*, **37**(125): 89–96.
- Colbeck, S.C.** (1982) Growth of faceted crystals in a snow cover. CRREL Report 82-29, U.S. Army Cold Regions Research and Engineering Laboratory, Hanover, N.H.
- Colbeck, S.C.** (1983) Theory of metamorphism of dry snow. *Journal of Geophysical Research*, **88**(C9): 5475–5482.
- Colbeck, S.C.** (1989) Air movement in snow due to windpumping. *Journal of Glaciology*, **35**(120): 209–213.
- Colbeck, S.C.** (1997) Model of wind pumping for layered snow. *Journal of Glaciology*, **43**(143): 60–65.
- Cunningham, J., and E.D. Waddington** (1993) Air flow and dry deposition of non-sea salt sulfate in polar firn: Paleoclimatic implications. *Atmospheric Environment, Part A*, **27**(17–18): 2943–2956.
- Davidson, C.I., M.H. Bergin, and H.D. Kuhns** (1996) The deposition of particles and gases to ice sheets. In *Chemical Exchange Between the Atmosphere and Polar Snow*, NATO ASI Series I, **43**: 275–306.
- Davis, R.E., E.M. Arons, and M.R. Albert** (1996) Metamorphism of polar firn: Significance of microstructure in energy, mass and chemical species transfer. In *Chemical Exchange Between the Atmosphere and Polar Snow* (E.W. Wolff and R.C. Bales, ed.), NATO ASI Series I, **43**: 379–401.

- Dibb, J. E., and M. Arsenault** (2002) Shouldn't snowpacks be sources of monocarboxylic acids? *Atmospheric Environment*, **36**(15–16): 2513–2521.
- Dibb, J.E., R.W. Talbot, J.W. Munger, D.J. Jacob, and S.M. Fan** (1998) Air–snow exchange of HNO₃ and NO_y at Summit, Greenland. *Journal of Geophysical Research*, **103**(D3): 3475–3486.
- Dibb, J.E., M.A. Arsenault, M.C. Peterson, and R.E. Honrath** (2002) Fast nitrogen oxide photochemistry in Summit, Greenland snow. *Atmospheric Environment*, **36**(15–16): 2501–2512.
- Gjessing, Y.T.** (1977) The filtering effects of snow. In *Isotopes and Impurities in Snow and Ice Symposium, 1975*, International Association of Hydrological Sciences Publications 118, p. 199–203.
- Gow, A.J.** (1968) Deep core studies of the accumulation and densification of snow at Byrd Station and Little America 5, Antarctica. Research Report 197, U.S. Army Cold Regions Research and Engineering Laboratory, Hanover, N.H.
- Gow, A.J.** (1969) On the rates of growth of grains and crystals in South Polar firn. *Journal of Glaciology*, **8**(53): 241–252.
- Gow, A.J.** (1971) Depth–time–temperature relationships of ice crystal growth in polar glaciers. Research Report 300, U.S. Army Cold Regions Research and Engineering Laboratory, Hanover, N.H.
- Gow, A.J., D.A. Meese, R.B. Alley, J.J. Fitzpatrick, S. Anandakrishnan, G.A. Woods, and B.C. Elder** (1997) Physical and structural properties of the Greenland Ice Sheet Project 2 ice core: A review. *Journal of Geophysical Research*, **102**(C12): 26559–26575.
- Harder, S.L., S.G. Warren, R.J. Charlson, and D.S. Covert** (1996) Filtering of air through snow as a mechanism for aerosol deposition to the Antarctic ice sheet. *Journal of Geophysical Research*, **101**(D13): 18729–18743.
- Hardy, J.P., and M.R. Albert** (1993) The permeability of temperate snow: Preliminary links to microstructure. *Proceedings of the 50th Annual Eastern Snow Conference, 8–10 June, 1993*, p. 146–156.
- Hoff, J.T., D. Gregor, D. Mackey, F. Wania, and C.Q. Jia** (1998) Measurement of the specific surface area of snow with the Nitrogen adsorption technique. *Environmental Science Technology*, **32**: 58–62.
- Honrath, R.E., M.C. Peterson, S. Gua, J.E. Dibb, P.B. Shepson, and B. Campbell** (1999) Evidence of NO production within or upon ice particles in the Greenland snowpack. *Geophysical Research Letters*, **26**(6): 695–698.

- Honrath, R.E., Y. Lu, M.C. Peterson, J.E. Dibb, M.A. Arsenault, N.J. Cullen, and K. Steffen** (2002) Vertical fluxes of NO_x, HONO, and HNO₃ above the snowpack at Summit, Greenland. *Atmospheric Environment*, **36**(15–16): 2629–2640.
- Hutterli, M.A., R. Rothlisberger, and R.C. Bales** (1999) Atmosphere-to-snow-to-firn transfer studies of HCHO at Summit, Greenland. *Geophysical Research Letters*, **26**(12): 1691–1694.
- Jones, A.E., R. Weller, P.S. Anderson, H.W. Jacobi, E.W. Wolff, O. Schrems, and H. Miller** (2001) Measurements of NO_x emissions from the Antarctic snowpack. *Geophysical Research Letters*, **28**: 1499–1502.
- Langham, E.J.** (1981) Physics and properties of snow cover. In *Handbook of Snow: Principles, Processes Management and Use*. Pergamon Press, Toronto, Canada, p. 275–337.
- Luciano, G.L., and M.R. Albert** (2002) Bi-directional permeability measurements of polar firn at Summit, Greenland. *Annals of Glaciology*, **35**: 63–66.
- Mellor, M.** (1975) A review of basic snow mechanics. Miscellaneous Paper 730, U.S. Army Cold Regions Research and Engineering Laboratory, Hanover, N.H.
- Nereson, N.A., E.D. Waddington, C.F. Raymond, and H.P. Jacobson** (1996) Predicted age-depth scales for Siple Dome and inland WAIS ice cores in West Antarctica. *Geophysical Research Letters*, **23**(22): 3163–3166.
- Perla, R.** (1982) Preparation of section planes in snow specimens. *Journal of Glaciology*, **28**(98): 199–204.
- Peterson, M., and R. Honrath** (2001) Observations of rapid photochemical destruction of ozone in snowpack interstitial air. *Geophysical Research Letters*, **28**: 511–514.
- Petit, J.R., I. Basile, A. Leruyet, D. Raymond, and C. Lorius** (1997) Four climate cycles in Vostok ice core. *Nature*, **387**(6631): 359–360.
- Revil, A., and L.M. Cathles** (1999) Permeability of shaly sands. *Water Resources Research*, **35**(3): 651–662.
- Schwander, J., B. Stauffer, and A. Sigg** (1988) Air mixing in firn and the age of the air at pore close off. *Annals of Glaciology*, **10**: 141–145.
- Schwander, J., J.M. Barnola, C. Andrie, M. Leuenberger, A. Ludin, D. Raynaud, and B. Stauffer** (1993) The age of air in the firn and ice at Summit, Greenland. *Journal of Geophysical Research*, **98**(D2): 2831–2838.

- Shimizu, H.** (1970) Air permeability of deposited snow. *Low Temperature Science*, Series A (22): 32.
- Sowers, T., M. Bender, D. Raynaud, and Y.S. Korotkevich** (1992) 15N of N_2 in air trapped in polar ice: A tracer of gas transport in the firn and a possible constraint in ice age–gas age differences. *Journal of Geophysical Research*, **97**(D14): 15683–15697.
- Sumner, A.L., and P.B. Shepson** (1999) Snowpack production of formaldehyde and its effect on the Arctic troposphere. *Nature*, 398, p.230-233.
- Swanson A.L., N.J. Blake, J.E. Dibb, M.R. Albert, D.R. Blake, and F.S. Rowland** (2002) Photochemically induced production of CH_3Br , CH_3I , $\text{C}_2\text{H}_5\text{I}$, ethene, and propene within surface snow at Summit, Greenland. *Atmospheric Environment*, **36**(15–16): 2671–2681.
- Waddington, E.D., J. Cunningham, and S.L. Harder** (1996) The effects of snow ventilation on chemical concentration. In *Chemical Exchange Between the Atmosphere and Polar Snow* (E.W. Wolff and R.C. Bales, ed.), NATO ASI Series I, **43**: 403–451.
- Waddington, E.D., E.J. Steig, and T.A. Neumann** (2002) Using characteristic times to assess whether stable isotopes in polar snow can be reversibly deposited. *Annals of Glaciology*, **35**: 118–124.

REPORT DOCUMENTATION PAGE

*Form Approved
OMB No. 0704-0188*

Public reporting burden for this collection of information is estimated to average 1 hour per response, including the time for reviewing instructions, searching existing data sources, gathering and maintaining the data needed, and completing and reviewing this collection of information. Send comments regarding this burden estimate or any other aspect of this collection of information, including suggestions for reducing this burden to Department of Defense, Washington Headquarters Services, Directorate for Information Operations and Reports (0704-0188), 1215 Jefferson Davis Highway, Suite 1204, Arlington, VA 22202-4302. Respondents should be aware that notwithstanding any other provision of law, no person shall be subject to any penalty for failing to comply with a collection of information if it does not display a currently valid OMB control number. PLEASE DO NOT RETURN YOUR FORM TO THE ABOVE ADDRESS.

1. REPORT DATE (DD-MM-YY) September 2004		2. REPORT TYPE Technical Report		3. DATES COVERED (From - To)							
4. TITLE AND SUBTITLE Microstructure of West Antarctic Firm and Its Effect on Air Permeability				5a. CONTRACT NUMBER							
				5b. GRANT NUMBER							
				5c. PROGRAM ELEMENT NUMBER							
6. AUTHOR(S) Ursula Rick and Mary Albert				5d. PROJECT NUMBER							
				5e. TASK NUMBER							
				5f. WORK UNIT NUMBER							
7. PERFORMING ORGANIZATION NAME(S) AND ADDRESS(ES) U.S. Army Engineer Research and Development Center Cold Regions Research and Engineering Laboratory 72 Lyme Road Hanover, NH 03755-1290				8. PERFORMING ORGANIZATION REPORT ERDC/CRREL TR-04-16							
9. SPONSORING/MONITORING AGENCY NAME(S) AND ADDRESS(ES) National Science Foundation				10. SPONSOR / MONITOR'S ACRONYM(S)							
				11. SPONSOR / MONITOR'S REPORT NUMBER(S)							
12. DISTRIBUTION / AVAILABILITY STATEMENT Approved for public release; distribution is unlimited. Available from NTIS, Springfield, Virginia 22161.											
13. SUPPLEMENTARY NOTES											
14. ABSTRACT The microstructure of snow and firm has a great impact on the transport of chemical species from the atmosphere to the underlying firm. For improved ice core interpretation, it is important to understand air-snow interactions within the firm layers and how they are affected by snow microstructure. Permeability and thick-section microstructure measurements have been made from snowpit and firm core samples retrieved during the U.S.-International Trans-Antarctic Science Expedition (ITASE) 1999-2001 field seasons. Our measurements have shown that the permeability of the snow at all of the sites generally increases with depth into the firm to about 3 m, then decreases due to microstructure changes, although at several sites there were areas of increased permeability at depth because of local changes in weather and climate. Thick-section microstructure measurements show that the grain size generally increases with depth, and the specific surface decreases with depth. Rapid grain growth is caused by diurnal and seasonal temperature gradients near the surface. Deeper in the core, the grain growth slows as the firm temperature gradients become small. The grain growth and specific surface trends do not follow those of the permeability. Pore size correlates well with the permeability of the snow samples; a formula was developed that predicts the firm permeability from pore characteristics. In addition to variation with depth in the core, the permeability and microstructure vary greatly from site to site, revealing that meteorological effects, such as accumulation rate and mean annual temperature, are important factors in shaping the firm microstructure. High accumulation rates or low mean annual temperatures will result in low permeability due to little or no metamorphism in the firm, although accumulation rate seems to be the dominant factor. Conversely, high mean annual temperatures cause faster grain growth, and low accumulation rates leave the near-surface firm exposed to temperature gradients for a longer time. Competing effects of temperature and accumulation rate can result in similar densities for sites of very different meteorological conditions. However, the permeability profile is a more sensitive indicator of meteorological condition than density. Physical characteristics of permeability and microstructure in the firm serve as climate indicators.											
15. SUBJECT TERMS <table style="width: 100%; border: none;"> <tr> <td style="text-align: center;">Antarctica</td> <td style="text-align: center;">Ice cores</td> <td style="text-align: center;">Permeability</td> </tr> <tr> <td style="text-align: center;">Firm</td> <td style="text-align: center;">Ice structure</td> <td></td> </tr> </table>						Antarctica	Ice cores	Permeability	Firm	Ice structure	
Antarctica	Ice cores	Permeability									
Firm	Ice structure										
16. SECURITY CLASSIFICATION OF:			17. LIMITATION OF OF ABSTRACT	18. NUMBER OF PAGES	19a. NAME OF RESPONSIBLE PERSON						
a. REPORT	b. ABSTRACT	c. THIS PAGE			19b. TELEPHONE NUMBER (include area code)						
U	U	U	U	88							